

Blacklock N, 2015, Vein characterization using structural controls and petrographic analysis at Cartier Zone in the Canadian Malartic property at Malartic, Quebec, BSc Thesis, Queen's U, ON, 68 p.

NSERC-CMIC Mineral Exploration Footprints Project Contribution 058.

Vein Characterization Using Structural Controls and Petrographic Analysis at Cartier Zone in the Canadian Malartic Property at Malartic, Quebec

Presented to
Faculty of Geological Sciences
And Geological Engineering
Queen's University

BSC. Thesis
April 17th 2015

Author:

Natalie Blacklock

Supervisors:

Gema Olivo, Queen's University

Stéphane Perrouty, University of Western Ontario

ABSTRACT

The Cartier Zone is located 4km northwest of the Canadian Malartic gold deposit. Host rock consists of Pontiac metasedimentary rocks, a quartz monzodiorite intrusion, and minor basic dykes composed of biotite, chlorite and carbonate with \pm quartz and \pm amphibole. Although the Cartier Zone exhibits multiple generations of veins and hydrothermal alteration the region is poorly mineralized in gold. The Cartier Zone underwent three deformation events: the first event (D_1) is observed only in the Pontiac metasedimentary rocks and is characterized by isoclinal folds. The second event (D_2) developed open to tight folds and a pervasive S_2 foliation while the third event (D_3) corresponds to large open folding of the S_2 foliation. Both the D_2 and D_3 events are observed in both the Pontiac metasedimentary rocks and the quartz monzodiorite intrusion. Eleven different vein systems were characterized and classified in chronological order due to cross cutting relationships observed at outcrop and by drill core logging. The first three vein systems, denoted as A, B, and C were observed only in the Pontiac metasedimentary rocks and formed pre- D_2 . Vein D occurred after the quartz monzodiorite intrusion emplacement and formed pre- to syn- D_2 . Vein systems E through I formed post- D_2 to pre- D_3 whereas Veins systems J through K formed Post- D_3 . Veins A, B, C and G are composed of quartz with minor proportions of \pm feldspar \pm biotite and \pm chlorite concentrated in the vein margin. Veins systems D, F, J are composed primarily of quartz and have minor proportions of carbonate concentrated in the selvage in Vein D and in the vein margin of Vein systems F and J. Vein systems E and I have distinct mineral compositions. Vein E is composed entirely of feldspar and forms an alteration selvage of feldspar, quartz and muscovite and Vein I contains equal proportions of quartz and tourmaline. Both Vein H and Vein K are comprised of quartz and pyrite where mineralization forms in the selvage of Vein H and in the vein margin of Vein K. Geochemical analyses revealed that Vein H forming in the quartz monzodiorite intrusion had the highest proportion of gold at 0.35ppm whereas the other remaining vein systems had gold values less than

0.006ppm. Comparisons were made to vein systems in the Canadian Malartic Deposit and due to similarities in mineral composition of the veins and associated alteration, Vein systems A to D appear to be associated with the early pre ore-stage veins, whereas Vein systems E to K are associated with the pre ore-stage veins seen at the Canadian Malartic Deposit.

ACKNOWLEDGEMENTS

This thesis would not have been possible without the help of a large group of individuals. I would like to thank NSERC-CMIC footprints project, specifically at the gold site for giving me the opportunity to participate in the PDAC and GAC-MAC conferences. I would also like to thank the Canadian Malartic exploration team for allowing me to work at the Canadian Malartic Mine site to collect my thesis material. As for specific individuals I would like to thank my supervisor Stéphane Perrouty for being an advisor to the project, assisting with the collect of research material and providing knowledge and data on the structure at Cartier Zone. I would also like to thank my primary supervisor Gema Olivo for providing me with valuable knowledge on detailed characterization concepts both in the field and in the laboratory for petrographic analysis.

TABLE OF CONTENTS

ABSTRACT	I
ACKNOWLEDGEMENTS	III
TABLE OF CONTENTS.....	IV
TABLE OF FIGURES	VI
TABLE OF TABLES	IX
1 INTRODUCTION	1
1.1 BACKGROUND AND PREVIOUS WORK.....	1
1.2 OBJECTIVES AND SCOPE	2
1.3 LOCATION OF OUTCROP AND ACCESS	2
2 REGIONAL GEOLOGY.....	3
2.1 TECTONIC SETTING.....	3
2.2 CANADIAN MALARTIC DEPOSIT	5
2.3 CARTIER ZONE: PREVIOUS STUDIES.....	10
3 METHODOLOGY.....	14
3.1 FIELD METHODS	14
3.2 GEOCHEMICAL ANALYSIS OF WHOLE ROCK SAMPLES FOR GOLD CONTENT	15
3.3 PETROGRAPHIC ANALYSIS.....	16
4 GEOLOGY OF CARTIER ZONE	17
4.1 ROCK UNITS	17
4.2 DEFORMATION.....	22

5	CHARACTERIZATION OF THE VEIN SYSTEMS.....	24
5.1	DETAILED MAPS	25
5.2	VEIN A.....	30
5.3	VEIN B.....	31
5.4	VEIN C.....	32
5.5	VEIN D	34
5.6	VEIN E	36
5.7	VEIN F	37
5.8	VEIN G	39
5.9	VEIN H	40
5.10	VEIN I.....	41
5.11	VEIN J	43
5.12	VEIN K.....	45
5.13	GOLD CONTENT	46
6	DISCUSSION.....	47
6.1	COMPARISON OF VEIN SYSTEMS.....	47
6.2	COMPARISON WITH PREVIOUS WORK AT CARTIER ZONE	50
6.3	COMPARISON TO THE CANADIAN MALARTIC DEPOSIT	51
7	CONCLUSION AND FURTHER WORK.....	54
8	REFERENCES	56

TABLE OF FIGURES

FIGURE 1: LOCATION OF THE CANADIAN MALARTIC DEPOSIT WITHIN THE ABITIBI GREENSTONE BELT. MODIFIED FROM DUBÉ AND GOSSELIN, (2007) AND (ROBERT, 1990).	3
FIGURE 2: MAP ILLUSTRATING LOCAL GEOLOGY OF THE PONTIAC SUBPROVINCE SOUTH OF THE CADILLAC TECTONIC ZONE AND THE SETTING OF THE CANADIAN MALARTIC DEPOSIT AND CARTIER ZONE HOSTED BY ROCKS OF THE PONTIAC GROUP AND PICHÉ GROUP. GEOLOGICAL MAP COMPILED BY S. PERROUTY (PERSONAL COMMUNICATION).	6
FIGURE 3: GEOLOGIC MAP OF CARTIER ZONE (NEUMAYR ET AL. 2000).....	13
FIGURE 4: EXAMPLE OF THE GRID SYSTEM USED TO COMPLETE THE DETAILED MAPS WHERE IMPORTANT CROSS CUTTING RELATIONSHIPS WERE OBSERVED.....	14
FIGURE 5: LOCATION AND ORIENTATION OF SELECTED DRILL HOLES PROJECTED TO SURFACE.	15
FIGURE 6: PHOTOMICROGRAPHS OF THE PONTIAC METASEDIMENTARY ROCKS ILLUSTRATING THE RELEVANT MINERALS AND TEXTURAL RELATIONSHIPS. A: (SAMPLE K389761) X-POLAR IMAGE OF THE TYPICAL PONTIAC GREYWACKE WITH FRAMEWORK GRAINS CONSISTING OF QUARTZ GRAINS AND CONGLOMERATES AS WELL AS ALTERED FELDSPAR GRAINS. B: (SAMPLE K389761) X-POLAR IMAGE OF THE MAJOR S_2 FOLIATION THAT IS DEFINED BY ELONGATE BIOTITE GRAINS. C: (SAMPLE K389763) PLANE LIGHT IMAGE OF THE GREYWACKE UNIT WHERE TWO GENERATIONS OF BIOTITE ARE PRESENT. HYDROTHERMAL BIOTITE THAT DEFINES THE FOLIATION REPLACES BIOTITE THAT WAS ORIGINALLY PART OF THE HOST ROCK. D: (SAMPLE K389762) PLANE LIGHT IMAGE SHOWING THE WEAK FOLIATION DEFINED BY THE ORIENTED BIOTITE GRAINS. E: (SAMPLE K389766) X-POLAR IMAGE OF CHLORITE AND BIOTITE AMYGDALOIDALS THAT ARE ORIENTED PARALLEL TO THE S_2 FOLIATION. F: (SAMPLE K389764) PLANE LIGHT IMAGE OF THE SILTSTONE WHERE LARGE EUHEDRAL PYRRHOTITE GRAINS OCCUR IN THE BIOTITE-RICH (IRON-RICH) BEDDING PLANES.....	19
FIGURE 7: (SAMPLE K389761) PLANE LIGHT PHOTOMICROGRAPH OF A PYRITE GRAIN THAT EXHIBITS A PRESSURE SHADOW THAT FORMED SYN- D_2 AS IT IS PARALLEL TO THE S_2 FOLIATION AND SHOWS SINISTRAL ROTATION.....	20
FIGURE 8: PHOTOMICROGRAPHS OF THE QUARTZ MONZODIORITE INTRUSION ILLUSTRATING THE RELEVANT MINERALS AND TEXTURAL RELATIONSHIPS. A: (SAMPLE K389810) X-POLAR IMAGE OF THE MOST UNALTERED SECTION OF THE INTRUSION WITH PLAGIOCLASE PHENOCRYSTS AND QUARTZ GROUNDMASS SHOWING MINOR CARBONATE REPLACEMENT. B: (SAMPLE K389815) X-POLAR IMAGE SHOWING SILICIFICATION OF THE GROUNDMASS AND REPLACEMENT OF THE PHENOCRYST MARGINS. C: (SAMPLE K389769) X-	

POLAR IMAGE OF ALTERATION AT THE CONTACT BETWEEN THE INTRUSION AND THE PONTIAC METASEDIMENTARY ROCKS IN THE FORM OF SILICIFICATION, PYRITIZATION, BIOTITE AND CHLORITE ALTERATION. D: (SAMPLE K389776) X-POLAR IMAGE SHOWING MUSCOVITE AND CARBONATE REPLACEMENT OF THE GROUNDMASS.	22
FIGURE 9: GEOLOGIC MAP OF CARTIER ZONE (COMPILED BY S. PERROUTY, PERSONAL COMMUNICATION).	23
FIGURE 10: INCORPORATING THE LARGE-SCALE STRUCTURAL FEATURES ONTO THE GEOLOGIC MAP AT CARTIER ZONE (COMPILED BY S. PERROUTY, PERSONAL COMMUNICATION).	24
FIGURE 11: LOCATION OF THE FOUR DETAILED MAPS AND FIGURES ILLUSTRATING KEY VEIN RELATIONSHIPS. GEOLOGICAL MAP COMPILED BY S. PERROUTY (PERSONAL COMMUNICATION).	25
FIGURE 12: DETAILED MAP A ILLUSTRATES CROSS CUTTING RELATIONSHIPS AMONGST THE VEIN SYSTEMS THAT FORMED PRE-D ₂ AND THE SIZE OF THE ALTERATION SELVAGE GENERATED BY THE 1MM SIZED E VEINLET. THE FOLIATION IS MORE INTENSE IN THIS LOCATION SO CROSS CUTTING RELATIONSHIPS WITH THE MAJOR S ₂ FOLIATION ASSISTED IN DETERMINING VEIN CHRONOLOGY.	26
FIGURE 13: DETAILED MAP B ILLUSTRATES THE CROSS CUTTING RELATIONSHIPS AMONGST SIX OF THE EIGHT VEIN SYSTEMS THAT OCCUR IN THE PONTIAC METASEDIMENTARY ROCKS. VEIN CHRONOLOGY WAS DETERMINED BY RELATIONSHIPS TO FOLIATION AND BEDDING FOR THE SYSTEMS OCCURRING PRE-D ₂ AND MORE ON CROSS CUTTING RELATIONSHIPS WITH OTHER VEINS FOR VEIN SYSTEMS THAT FORMED POST-D ₂	27
FIGURE 14: DETAILED MAP C EXAMINES THE VEIN D SYSTEM EXCLUSIVELY TO SHOW HOW THE DEFORMATION OF THE VEINS FORM PARALLEL TO S ₂ FOLIATION THAT OCCURRED IN THE QUARTZ MONZODIORITE INTRUSION.	28
FIGURE 15: DETAILED MAP D ILLUSTRATES THE INTERACTION BETWEEN FIVE OF THE EIGHT VEIN SYSTEMS THAT OCCUR IN THE QUARTZ MONZODIORITE INTRUSION. SURFACE WEATHERING GENERATED VUGGY CAVITIES IN THE VEIN H SYSTEMS AND AN OXIDIZED SELVAGE SURROUNDING THE VEIN J SYSTEM.	29
FIGURE 16: VEIN A TRANSPOSED ALONG S ₂ CROSSCUT BY VEIN H.....	30
FIGURE 17: PHOTOMICROGRAPHS OF THE VEIN A SYSTEM ILLUSTRATING THE RELEVANT MINERALS AND TEXTURAL RELATIONSHIPS. A. (SAMPLE K389763) X-POLAR IMAGE OF THE FIRST SUBTYPE SHOWING THE SHARP CONTACT BETWEEN THE VEIN AND PONTIAC METASEDIMENTARY HOST ROCK WHERE FELDSPAR CRYSTALLIZES IN THE VEIN MARGIN AND REPLACES THE QUARTZ GRAINS. B. (SAMPLE K389762) PLANE LIGHT IMAGE OF THE SECOND SUBTYPE SHOWING THE CONTACT BETWEEN THE VEIN AND HOST ROCK WHERE FINE GRAINED FELDSPAR AND BIOTITE FORM IN THE VEIN MARGIN/SELVAGE.	31

FIGURE 18: (SAMPLE K389762) PLANE LIGHT PHOTOMICROGRAPH OF THE VEIN B SYSTEM ILLUSTRATING THE SHARP CONTACT BETWEEN VEIN B AND THE PONTIAC METASEDIMENTARY HOST ROCK WHERE FE-CHLORITE FORMS IN THE VEIN MARGIN. 32

FIGURE 19: VEIN C WITH SHALLOW DIP WAS DEFORMED BY THE D₂ EVENT. 33

FIGURE 20: PHOTOMICROGRAPHS OF THE VEIN C SYSTEM ILLUSTRATING THE RELEVANT MINERALS AND TEXTURAL RELATIONSHIPS. A: (SAMPLE K389764) PLANE LIGHT IMAGE OF CHLORITE OVERPRINTING FELDSPAR IN THE VEIN MARGIN. B: (SAMPLE K389764) X-POLAR IMAGE OF THE QUARTZ RICH ALTERATION SELVAGE WHERE BIOTITE FROM THE ORIGINAL HOST ROCK IS PRESERVED IN THE SELVAGE. 34

FIGURE 21: PHOTOMICROGRAPHS AND FIELD OBSERVATIONS OF THE VEIN D SYSTEM ILLUSTRATING THE RELEVANT MINERALS AND TEXTURAL RELATIONSHIPS. A: IMAGE FROM THE OUTCROP SHOWING 1MM CARBONATE ALTERATION IN THE SELVAGE. B: (SAMPLE K389810) X-POLAR IMAGE OF THE SUTURED CONTACT BETWEEN QUARTZ GRAINS. C: (SAMPLE K389810) X-POLAR IMAGE OF CARBONATE AND MUSCOVITE ALTERATION THAT REPLACES QUARTZ AT THE GRAIN MARGINS. D: (SAMPLE K389810) X-POLAR IMAGE OF THE SHARP CONTACT BETWEEN THE VEIN AND HOST ROCK. 35

FIGURE 22: (SAMPLE K389762) X-POLAR PHOTOMICROGRAPH OF THE VEIN E SYSTEM SHOWING THE SHARP CONTACT BETWEEN THE VEIN WHICH EXHIBITS INTER-FINGERING OF FELDSPAR GRAINS AND THE HOST ROCK THAT WAS REPLACED BY QUARTZ, FELDSPAR AND MUSCOVITE IN THE ALTERATION SELVAGE. 37

FIGURE 23: PHOTOMICROGRAPHS OF THE VEIN F SYSTEM ILLUSTRATING THE RELEVANT MINERALS AND TEXTURAL RELATIONSHIPS. A: (SAMPLE K389855) X-POLAR IMAGE OF THE SUTURED TEXTURE BETWEEN QUARTZ GRAINS IN THE INTRUSION. B: (SAMPLE K389855) X-POLAR IMAGE OF CARBONATE REPLACING THE QUARTZ CRYSTALS IN THE INTRUSION. C: (SAMPLE K389860) PLANE LIGHT IMAGE OF THE VEIN MARGIN WHERE CARBONATE SHOWS MINOR REPLACEMENT OF BIOTITE IN THE PONTIAC METASEDIMENTARY HOST ROCK. 38

FIGURE 24: IMAGE TAKEN FROM THE SOUTHWEST REGION OF THE OUTCROP WHERE THE COMPOSITE VEIN G SYSTEM WAS MOST PREVALENT. OXIDATION OCCURS IN THE VEIN MARGIN WHILE A 3MM THICK BLEACHED ALTERATION HALO FORMS IN THE SELVAGE. VEIN G IS CROSS CUT BY THE VEIN J SYSTEM. 39

FIGURE 25: PHOTOMICROGRAPHS AND FIELD OBSERVATIONS OF THE VEIN H SYSTEM ILLUSTRATING THE RELEVANT MINERALS AND TEXTURAL RELATIONSHIPS. A: IMAGE FROM OUTCROP SHOWING PYRITE WEATHERING THAT FORMED BOXWORK TEXTURE. B: (SAMPLE K389774) X-POLAR IMAGE OF EMBAYED QUARTZ GRAINS IN THE VEIN. C: (SAMPLE K389774) X-POLAR IMAGE OF FINE-GRAINED QUARTZ THAT OCCURS WITH PYRITE IN THE VEIN MARGIN. 41

FIGURE 26: VEIN I WAS OBSERVED IN THE CENTRAL REGION OF THE QUARTZ MONZODIORITE INTRUSION CROSS CUTTING VEIN D WHERE TOURMALINE IS OBSERVED AT THE VEIN MARGIN.42

FIGURE 27: (SAMPLE K389771) X-POLAR PHOTOMICROGRAPH OF THE VEIN I SYSTEM ILLUSTRATING THE RELATIONSHIP BETWEEN THE QUARTZ AND TOURMALINE IN THE VEIN. BOTH QUARTZ AND TOURMALINE FORMED IN THE SAME TIME FRAME SINCE TOURMALINE FORMS AS INCLUSIONS IN THE QUARTZ WHILE OTHER TOURMALINE GRAINS MAKE SHARP CONTACT WITH THE QUARTZ.43

FIGURE 28: IMAGE OF VEIN J IN THE INTRUSION SHOWING THE COMPOSITE SETS ORIENTED 275°/90 AND 300°/65 CROSS CUTTING THE VEIN G SYSTEM. SURFICIAL WEATHERING FORMED THE OXIDIZED VUGGY CAVITIES.44

FIGURE 29: PHOTOMICROGRAPHS OF THE VEIN J SYSTEM ILLUSTRATING THE RELEVANT MINERALS AND TEXTURAL RELATIONSHIPS. A: (SAMPLE K389815) X-POLAR IMAGE OF THE SHARP CONTACT BETWEEN THE QUARTZ RICH VEIN AND THE QUARTZ MONZODIORITE HOST ROCK. B: (SAMPLE K389776) X-POLAR IMAGE OF ALTERATION ATTRIBUTED TO THE VEIN J SYSTEM WHERE CARBONATE AND BIOTITE REPLACEMENT OF THE PLAGIOCLASE PHENOCRYSTS.45

FIGURE 30: CHRONOLOGICAL SEQUENCE OF THE ELEVEN VEIN SYSTEMS FOUND AT THE CARTIER ZONE. VEINS A-C ARE DENOTED BY HATCH LINES DUE TO THE LACK OF EVIDENCE TO CONSTRAIN THE VEIN SYSTEMS WITH EITHER THE D₁ EVENT OR THE INTRUSION EMPLACEMENT.47

FIGURE 31: VEIN CHRONOLOGY AT CARTIER ZONE, COMPARING WITH THE VEIN SYSTEMS THAT WERE CHARACTERIZED PREVIOUSLY.51

TABLE OF TABLES

TABLE 1: CHARACTERISTICS AND STRUCTURAL TIMING OF QUARTZ VEIN SYSTEMS AT CARTIER ZONE (NEUMAYR ET AL. 2000).13

TABLE 2: PROPORTION OF GOLD IN SELECTED VEIN SYSTEMS DETERMINED BY AQUA REGIA ICP AND AU FIRE ASSAY INNA ANALYSIS.46

1 INTRODUCTION

1.1 BACKGROUND AND PREVIOUS WORK

Cartier Zone is a region of exposed outcrop approximately 4200m² in size and is located in a poorly mineralized part of the Canadian Malartic footprint. Host rock consist of Pontiac metasedimentary rocks which were intruded by a quartz monzodiorite intrusion and minor basic dykes composed of biotite, chlorite, carbonate with ± quartz and ± amphibole. Complex systems of veins were observed in both the Pontiac metasedimentary rocks and the intrusion and the entire region shows evidence of having undergone three separate folding events (Neumayr et al., 2000). Cartier Zone has been a location for prospective gold exploration since the early 20th century when the Malartic Deposit was discovered. The Cartier Malartic mine was an underground mining system established at the boundary between Malartic and Fournière Township. Preliminary work was completed at the outcrop between 1923 and 1927. In 1928 Cartier Malartic Gold Mines sunk a shaft with the belief that the zone was mineralized due to similarities to the Canadian Malartic Deposit however, operations were discontinued later that year and no gold was extracted (Gunning & Ambrose, 1940).

Previous work was completed at Cartier Zone, both on a regional scale and at outcrop scale. Conclusions from work completed by Gunning and Ambrose (1940) and Neumayr et al. (2000) suggested that Cartier Zone had experienced three stages of deformation and the main alteration feature was a system of folded quartz veins that occur in the quartz monzodiorite intrusion. Neumayr et al. (2000) went further to characterize five systems of quartz veins at the outcrop. Since the style of mineralization at the Canadian Malartic Deposit is in either disseminated or in fine veinlets (Helt et al., 2014), it is necessary to investigate the alteration associated with the vein systems at Cartier Zone to evaluate if there is evidence as to why the region is poorly mineralized.

1.2 OBJECTIVES AND SCOPE

This thesis is part of a larger five-year project that aims to develop a robust mineralogical, geochemical, petrophysical and geophysical model of the Canadian Malartic gold deposit footprint. The objectives of this thesis are to:

- a) Characterize the vein systems by establishing the major structural controls, mineralogy and wall-rock alteration in the Cartier Zone and to determine their paragenesis.
- b) Compare vein systems and alteration features of Cartier Zone to the Canadian Malartic Deposit and its footprint.

This study was completed in two parts: 1) Field work was completed at Cartier Zone of the Canadian Malartic Property, in Malartic Quebec in the summer of 2014 as part of a Natural Sciences and Engineering Research Council (NSERC) and the Canadian Mining Innovation Council (CMIC) research project. 2) Petrographic, mineralogical and geochemical investigations were completed from August 2014 to March 2015 in the Dr. Olivo Petrographic Laboratory at Queen's University.

1.3 LOCATION OF OUTCROP AND ACCESS

The Cartier Zone occurs 4km northwest of Malartic, Quebec. Canadian Malartic Mine provided access to the site for the 2014 field season through their exploration office branch and their exploration trucks were used for daily transport to the site.

2 REGIONAL GEOLOGY

2.1 TECTONIC SETTING

Canadian Malartic occurs at the boundary between the Abitibi subprovince to the north and Pontiac subprovince to the south. The Cadillac-Larder Lake tectonic zone separates these subprovinces, which is a domain of steeply dipping NW-SE trending major faults north of Cartier Zone (Robert, 1989). Cartier Zone is situated in the Pontiac subprovince and occurs 500m south of the Cadillac tectonic zone (Neumayr et al., 2000). The contact between the subprovinces is marked by the tectonic fault zone that stretches 300km from Timmins, Ontario to Val D'Or Quebec (Figure 1). The Cadillac tectonic zone also acts as a lithological boundary between the Abitibi Greenstone to the north and the metasedimentary rocks of the Pontiac Group to the south. Piché Group metavolcanic rocks found at Canadian Malartic are restricted to the Cadillac tectonic zone (Desrochers & Hubert, 1996).

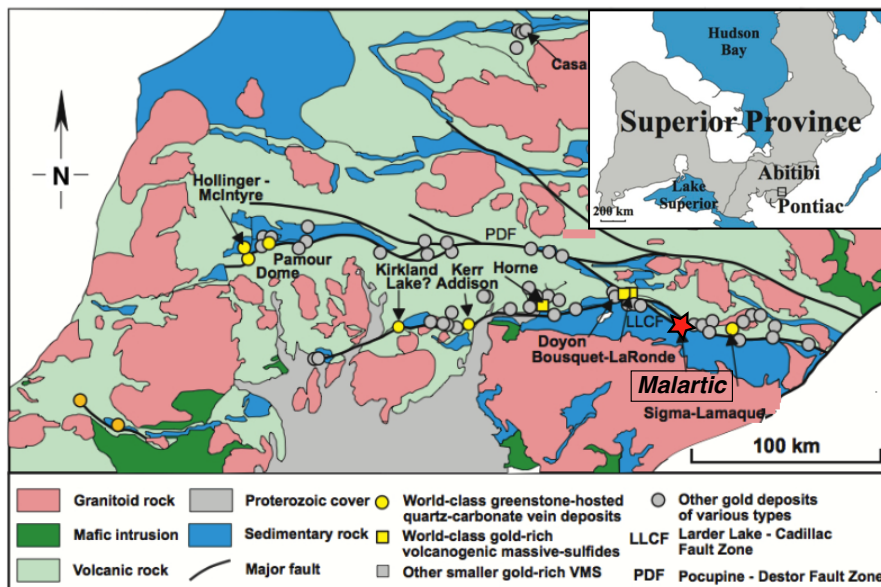


Figure 1: Location of the Canadian Malartic Deposit within the Abitibi Greenstone Belt. Modified from Dubé and Gosselin, (2007) and (Robert, 1990).

Several papers have been published on the geochronology of the southern Abitibi greenstone belt and the Pontiac subprovince near the Cadillac-Larder lake tectonic zone. Work by Corfu (1993) using Zircon U-Pb geochronology showed that the Abitibi greenstone belt developed between 2750Ma and 2670Ma. Of this early igneous activity, major pre-orogenic magmatism was confined mainly to the period of 2720Ma to 2700Ma (Corfu, 1993). The later calc-alkaline plutons occurred between 2694Ma and 2690Ma (Corfu, 1993; Corfu, et al. 1989) and the later plutonium was associated with the deposition of alluvial-fluvial sequences between 2696Ma and 2687Ma (Davis, 1992). Later uplift and erosion led to the deposition of conglomerates and fluvial sandstones were deposited between 2680Ma and 2672Ma as part of the Timiskaming Event, creating an unconformity with the underlying volcanic pluton assemblages (Corfu, 1993).

Similar work was conducted in the Pontiac subprovince in the Pontiac metasedimentary rocks south of the Cadillac-Larder lake tectonic zone. Work by Davis (2002) examined U-Pb ages from individual detrital zircons from the northern part of the Pontiac subprovince and from the Cadillac, Kewagama and Lac Caste Groups within the southern Abitibi subprovince. Results showed that the youngest detrital zircons formed between 2693Ma and 2685Ma (Davis D. , 2002). The age for the Lac Fournière intrusion in the Pontiac subprovince was dated at $2682 \pm 1\text{Ma}$, which constrains the minimum age of the Pontiac metasedimentary rocks. The monzodiorite intrusion that occurs at the Canadian Malartic Deposit south of the Cadillac-Larder lake tectonic zone was dated between 2677Ma to 2679Ma (Helt et al., 2014) and correlates to ages reported previously between 2680Ma and 2676Ma by Corfu et al. (1989) and Davis et al. (2000) elsewhere in the Pontiac subprovince. Correlation between other dominantly alkalic, felsic to intermediate intrusions suggest that the monzodiorite intrusion at Canadian Malartic Deposit may be contemporaneous with the intrusion at Cartier Zone.

Three major deformation events (referred to as D_{1-3}) were associated with the evolution of the Pontiac subprovince (Robert, 2001). The Malartic Composite Block, used to describe the structural domains surrounding the Malartic deposit by Desrochers and Hubert (1996), underwent at least two phases of deformation. D_1 was associated with the tilting, folding and thrusting that occurred between 2687Ma and 2672Ma (Sanfaçon & Hubert, 1990) and the event produced ductile thrust faults and folds in the mafic and ultramafic domains (Desrochers and Hubert, 1996). In the Pontiac metasedimentary rocks the D_2 event occurred in 2680Ma and generated the regional E-W foliation that is observed at the Malartic Composite Block. The final deformation event D_3 produced small local conjugate kink folds that generated an E-W shortening (Desrochers and Hubert, 1996).

Regional metamorphism varies in the Pontiac subprovince from sub-greenschist to amphibolite facies, increasing in grade towards the S-SW (Desrochers & Hubert, 1996). The regional metamorphism overprints the entire region and occurred between 2677Ma and 2643Ma (Powell et al. 1995).

Retrograde metamorphism occurs throughout the Malartic Composite Block in the form of biotite that is retro-morphosed into chlorite and is most prevalent proximal to the Cadillac-Larder Lake tectonic zone (Desrochers & Hubert, 1996). The Cadillac tectonic zone became the central area of hydrothermal activity and gold deposition in second and third order shear zones.

2.2 CANADIAN MALARTIC DEPOSIT

Canadian Malartic Deposit has current reserves of 10.9 Moz of gold (Wares & Burzynski, 2012) and is the first bulk tonnage gold mine from the Superior Province (Helt et al., 2014). Originally the Canadian Malartic Deposit was a system of underground mining operations that were converted into an open pit in 2009 (Wares & Burzynski, 2012). It is an example of a large-tonnage low-grade deposit with a gold grade of 1.02 g/t Au (Helt et al., 2014).

The Canadian Malartic Deposit is in the Pontiac subprovince immediately south of the Malartic tectonic zone, which is a subdivision of the larger Cadillac Larder Lake tectonic zone (Figure 2). The structure associated with the Malartic tectonic zone is consistent with the D₂ event described by Desrochers and Hubert (1996) and is defined by two major E-W trending faults: Malartic fault to the north and Sladen fault to the south.

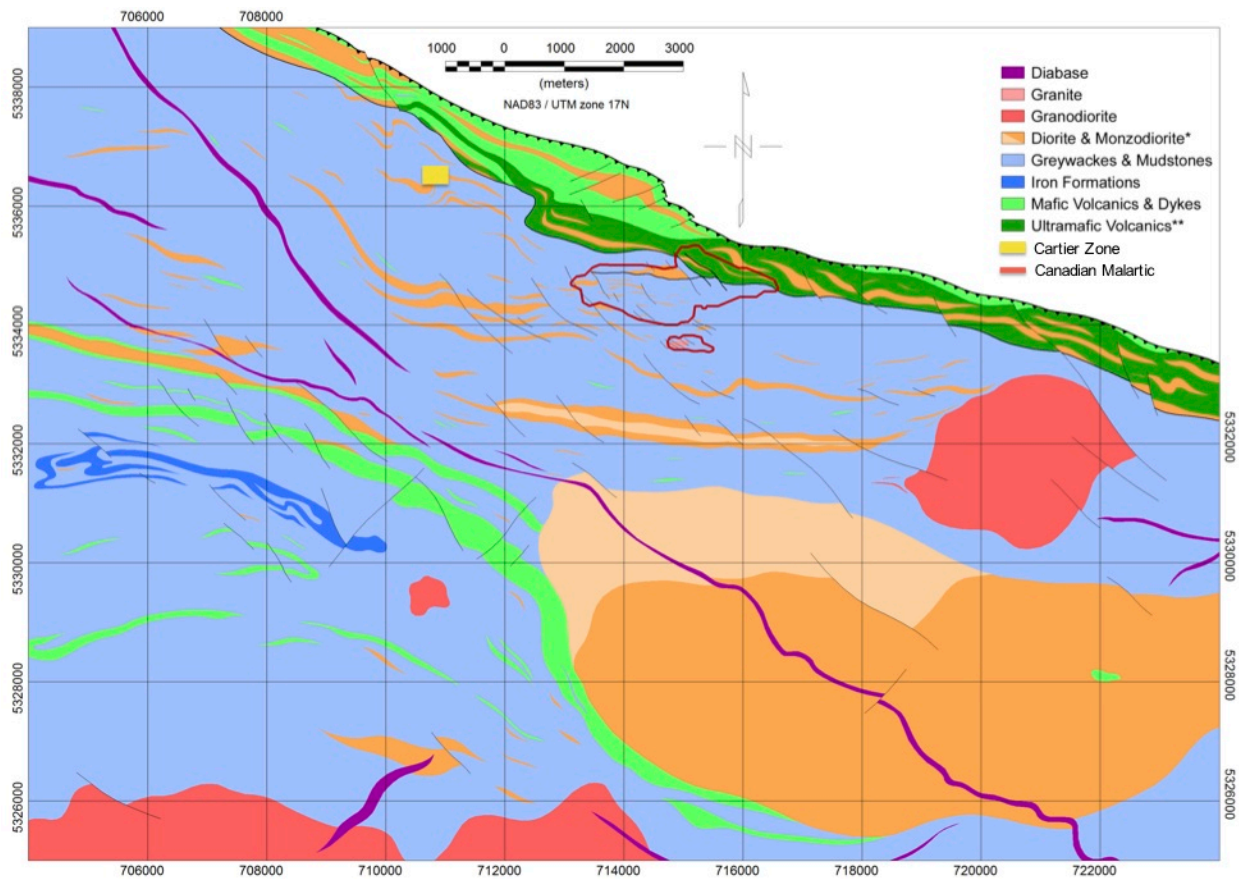


Figure 2: Map illustrating local geology of the Pontiac subprovince south of the Cadillac Tectonic Zone and the setting of the Canadian Malartic Deposit and Cartier Zone hosted by rocks of the Pontiac Group and Piché Group. Geological map compiled by S. Perrouty (personal communication).

2.2.1 Rock Units

At the Canadian Malartic Deposit the geology is comprised of metasedimentary rocks of the Pontiac Group, which overlay metavolcanic rocks of the Piché Group and a collection of monzodiorite intrusions. The bulk of the Canadian Malartic Deposit is located south of the Malartic tectonic zone and is hosted by Pontiac metasedimentary rocks and felsic to intermediate porphyritic intrusions (Robert, 1997).

2.2.1.1 Pontiac metasedimentary Rocks

Pontiac metasedimentary rock assemblage is comprised of quartz-rich greywacke and siltstone units that display a north to south decrease in bed thickness (Lajoie and Ludden, 1984). The Pontiac metasedimentary rocks are turbiditic clastic and form in rhythmically layered in beds ranging from 1mm to 1m in thickness. The Pontiac metasedimentary rocks were metamorphosed and show a well-developed foliation associated with the regional D₂ event. They range in colour from dark grey to black and are brown proximal to porphyry intrusions where hydrothermal biotite develops (Helt et al, 2014).

2.2.1.2 Piché Metavolcanic Rocks

Piché metavolcanic rocks consist of magnesian basaltic to komatiitic volcanic rocks that are strongly deformed. The volcanic rocks underwent hydrothermal alteration, characterized biotite replacement and carbonatization. In addition the Piché metavolcanic rock units are crosscut by several veinlets composed of talc, carbonate and chlorite (Sansfaçon and Hubert, 1990).

2.2.1.3 Felsic-Intermediate Porphyries

Felsic to intermediate porphyry systems intrude into the Piché metavolcanic rocks and the Pontiac metasedimentary rocks at the Canadian Malartic Deposit. The monzodiorite intrusions that are emplaced are associated with gold mineralization (Wares & Burzynski, 2012). The intrusions at the deposit range from subalkaline to transitional and are between dacitic to andesitic and trachyandesitic in chemical composition (Winchester and Floyd, 1977), (De Souza, 2014).

2.2.2 Alteration and Gold Mineralization

Each of the rock units at the Canadian Malartic Deposit have undergone pervasive alteration in the form of carbonatization, pyritization, silicification and extensive potassium feldspar, biotite, and muscovite replacement (Helt et al., 2014). Each of the vein systems experienced carbonatization, suggesting that carbonate alteration was extensive and occurred throughout the formation of the deposit (Helt et al., 2014).

Early, pre-ore stage veining is characterized by quartz with minor albite and carbonate, mainly calcite. The early stage alteration replaced the groundmass of the monzodiorite porphyry and the matrix of the Pontiac metasedimentary greywacke with fine-grained quartz and carbonate.

The pre-ore stage alteration produced vein-related biotite and potassium feldspar replacement with calcite and \pm pyrite alteration haloes around quartz, quartz-carbonate \pm biotite and quartz-carbonate-albite veinlets. Pervasive biotite alteration from the pre ore-stage veins overprints the early ore-stage alteration and minor chlorite is replaced by biotite in the Pontiac Metasedimentary rock (Helt et al. 2014). Pyrite associated with the biotite and feldspar alteration and occurs in the intrusion as disseminated grains in the mineralized veinlets (Helt et al., 2014).

Alteration from the Main ore-stage is associated with gold mineralization at the Canadian Malartic Deposit and formed local stockwork breccias of mm-cm scale veins of quartz/calcite \pm pyrite veins (De Souza, 2014). In addition, pegmatitic veins that formed during the main ore-stage are gold bearing and comprised of quartz, calcite, muscovite and biotite with trace amounts of albite, tourmaline, pyrite, galena and scheelite (De Souza, 2014). Mineralization in the monzodioritic intrusions consists of zones silicification and biotite alteration with alteration halos composed of carbonate and hematite (De Souza, 2014), whereas mineralization in the Pontiac metasedimentary rock occurs within alteration halo and is

comprised of disseminated pyrite, biotite and potassium feldspar alteration, carbonatization and sericitization (Helt et al. 2014).

The mineralized monzodioritic intrusions trend E-W and NW-SE and influenced the geometry of the Sladen fault that runs E-W throughout the deposit (De Souza, 2014). Gold is economically concentrated along the Sladen Fault, in the hinge zones of folds and along brittle-ductile deformation corridors running NW-SE (Sanfaçon & Hubert, 1990).

Late ore-stage veins contain coarse-grained quartz with porphyritic crystals of muscovite and biotite as well as finer grained crystals of pyrite and calcite. Alteration associated with the veins overprint the main ore-stage alteration with chloritization in both the intrusion and the Pontiac metasedimentary rocks (Helt et al., 2014).

2.2.3 Genetic Model

Work completed by Helt et al. (2014) examined the origin of gold mineralization to develop a genetic model for the Canadian Malartic Deposit using physicochemical constraints such as pressure, temperature, fugacity and pH on minerals in the Fe-O-S system. Results from the analysis led to the interpretation that a CO₂ and SO₂ bearing felsic magma, emplaced at mid-crustal levels, exsolving an oxidized and sulfur-rich ore fluid. The pH was buffered to higher values by carbonate alteration that depleted CO₂ in the fluid and resulted in an altered assemblage of potassium feldspar, quartz, biotite, calcite, ankerite and pyrite. Gold was transported as a bisulfide complex and was deposited at ~475°C (Helt et al., 2014), mainly as a result of sulfidation of the host rocks which replaced iron-bearing silicate minerals and destabilized the gold-bisulfide complexes (Helt et al., 2014). From these results the Canadian Malartic Deposit was interpreted to be intrusion-related since the gold mineralization was spatially related to the porphyritic intrusion and Helt et al. (2014) goes further to disprove the theory of

a porphyritic model since there was no evidence that the ore fluid exsolved from a shallowly emplaced porphyritic intrusion.

The term intrusion-related was originally used to classify a larger spectrum of styles of gold mineralization in epizonal to mesozonal environments (Robert, 1990). Helt et al. (2014) believes that Canadian Malartic is an example of an 'oxidized intrusion related' deposit and has connections to the syenite model proposed by Robert (2001).

2.3 CARTIER ZONE: PREVIOUS STUDIES

2.3.1 Tectonic Setting

Work completed by Gunning and Ambrose (1940) showed that the Malartic area straddles the Cadillac Tectonic Zone with Piché metavolcanic rocks extending to the north and Pontiac metasedimentary rocks extending to the south. The Cartier Zone is part of the Canadian Malartic property occurring in the Pontiac metasedimentary rocks 1km south of the larger Cadillac Larder Lake tectonic zone (Neumayr et al., 2007).

Two sets of folds were identified at Cartier Zone. The bedding (S_0) in the Pontiac metasedimentary rocks is folded about mesoscopic, upright and tight isoclinal folds (Neumayr et al., 2000). Field evidence showed that the porphyry intrusion took place after preliminary deformation in the Pontiac metasedimentary rocks. This was interpreted based on clear cross cutting relationships between the folded beds and the intrusion (Gunning & Ambrose, 1940).

The outcrop is situated at the hinge of a major fold that was identified using younging direction techniques such as cross bedding in the siltstone layers as well as graded bedding between the siltstone and greywacke units that make up the Pontiac metasedimentary rocks (Gunning & Ambrose, 1940).

Pervasive S_2 foliation, generated by the D_2 event, was defined by the parallel alignment of biotite in the

Pontiac metasedimentary rocks and by feldspar and quartz in the porphyry intrusion (Neumayr et al., 2000). Boudinaged S_2 -parallel porphyry dykes indicate ductile deformation along the shear zone and trend NW-SE to E-W. Both S_0 and the S_2 foliation are folded by a megascopic, moderately E-plunging F_3 fold (Neumayr et al., 2000).

The specific metamorphic grade of the outcrop was not identified due to the absence of critical mineral assemblages (Neumayr et al. 2000) however, work completed by Sansfaçon and Hubert (1990) determined amphibolite facies metamorphic grade 3km south of the outcrop. Since it is understood that there is an increasing metamorphic grade to the S-SW in the Pontiac subprovince (Desrochers & Hubert, 1996) the metamorphic grade is between sub-greenschist to amphibolite.

2.3.2 Rock Units

2.3.2.1 Pontiac Metasedimentary Rocks

At the time of the work completed by Gunning and Ambrose (1940), the sediments were interpreted to be part of the Kewagama Group, however this was corrected to the Pontiac Group by Neumayr et al. (2000). The Pontiac metasedimentary rocks at Cartier Zone are composed coarse-grained greywackes and fine-grained siltstones, which locally contain cross bedding and graded bedding (Neumayr et al, 2000). The bedding (S_0) within the Pontiac metasedimentary rocks strike NNW to W and dip moderately WSW to S and pervasive S_2 foliation that is defined by the parallel alignment of biotite strike WNW to NNW and dip steeply NNE to moderately ENE (Neumayr et al, 2000).

2.3.2.2 Quartz Monzodiorite Intrusion

Gunning and Ambrose (1940) described the intrusion as greyish-brown, fine-medium grained albite granite that occurs both as a porphyry intrusion in addition to several offset dyke systems. Modal composition of the intrusion was 50% albite (An₃), 20% quartz, 10-15% microcline, and trace amounts of various ferromagnesian minerals making it a quartz monzodiorite (Gunning & Ambrose, 1940).

2.3.3 Alteration and Vein Systems

Gunning and Ambrose (1940) described the main vein system as white vitreous veins composed of coarse-grained quartz that strike at right angles to the contact of the intrusive. The veins dip towards the east-northeast and can vary greatly in magnitude. There were also irregular bodies of quartz identified at the site that had no defined orientation (Gunning & Ambrose, 1940).

Quartz veins at the site were found to be barren in gold and had trace amounts of sulfides. Pyrite was more abundant in the surrounding porphyry than the vein systems. Some quartz veins had trace amount of galena, chalcopyrite, ankerite and tourmaline whereas small veinlets of chlorite, biotite and muscovite were also observed to cross cut the porphyry (Gunning & Ambrose, 1940).

Work that was completed by Neumayr et al. (2000) examined the Cartier Zone in more detail and developed a chronology for each of the different vein systems (Table 1). Based on structural setting and overprinting relationships, five different quartz vein types were identified (Figure 3). The nomenclature for the vein systems corresponds to the timing of deformation. The NW-trending shear zone along the F_3 fold limb hosts the boudinaged V2 quartz veins. V3A quartz veins are parallel to S_2 foliation, which is folded about the F_3 folds, and correspond to the vitreous quartz veins described by Gunning and Ambrose (1940). The V3B quartz/tourmaline and V3C quartz veins are hosted in the shear zones, which deformed V3A quartz veins. The E-W, N-S trending fracture set within the Pontiac metasedimentary rocks hosts a conjugate set of V3D quartz veins. Veins denoted as V2/3 are within the boudinaged porphyry (Neumayr et al., 2000).

Pyrite and galena occur within all vein types. However, most of the sulfides are hosted in the wall rocks adjacent to V2 and V3A veins. The V3B and V3C veins contain sulfides within the veins and wall rock (Neumayr et al., 2000).

Table 1: Characteristics and structural timing of quartz vein systems at Cartier Zone (Neumayr et al. 2000).

Vein	Structural setting	Width	Vein minerals	Mineralization	Timing			
					D ₁	D ₂	D ₃	
							early	late
V2	S ₂ parallel within NW-trending shear zone, boudinaged, sigmoidal	Several cm	Qtz	Py		?		
V3A	Folded about F ₃ folds, rods in the fold hinge of F ₃ folds	Up to 30 cm	Qtz	Py, ± Gn, Au				?
V3B	Hosted in E-W-trending D ₃ shear zone, deform V3A veins	Up to 15 cm	Qtz, Tur	Py, Au				
V3C	Same as V3B veins	Up to 10 cm	Qtz	Py, Au				
V3D	Hosted within conjugate fracture set in Pontiac rocks	1–2 cm	Qtz	Py				
V2/3	Within boudinaged porphyry dykes, openly folded	Up to 5 cm	Qtz		?			?

Notes: Au, gold; Gn, galena; Qtz, quartz; Py, pyrite; Tur, tourmaline.

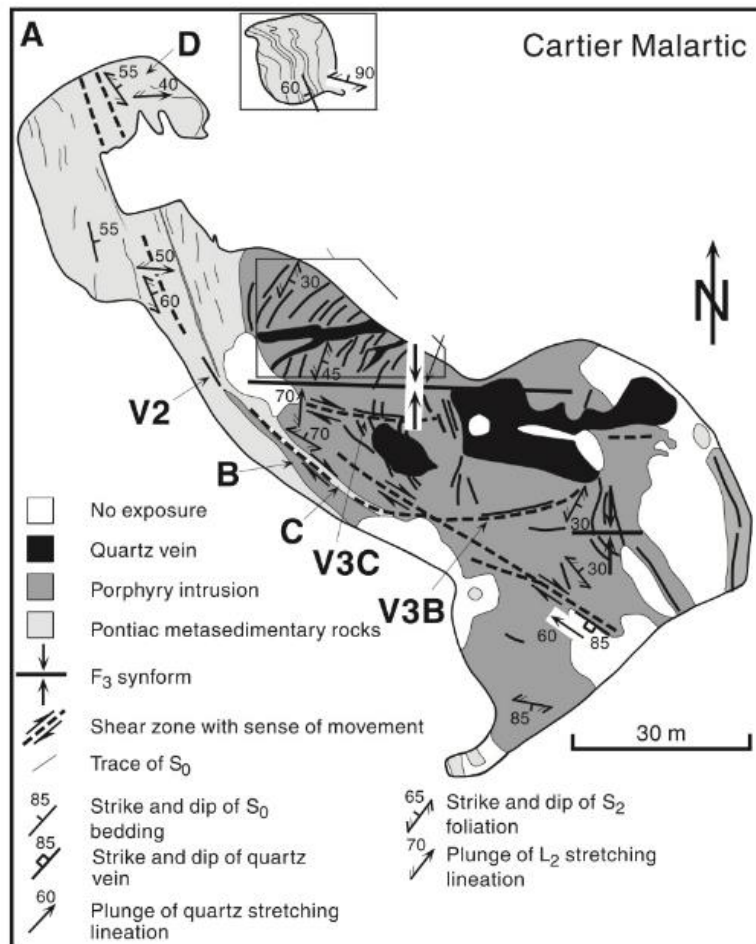


Figure 3: Geologic Map of Cartier Zone (Neumayr et al. 2000).

3 METHODOLOGY

3.1 FIELD METHODS

Vein mapping was completed at Cartier Zone and was used to determine structural controls that constrain the vein systems. Local structural controls were determined using crosscutting relationships between bedding, foliation(s), intrusion emplacement, and crosscutting relationships with other vein systems and were illustrated using small scale (1x1m) detailed maps (Figure 4). Four detailed sketches were completed at Cartier Zone. Outcrop observations were correlated with samples taken from drill core to identify the mineral assemblage and examine the extent of hydrothermal alteration from the vein systems. Selected drill holes CYGO9-2173 and CA14-2477 of the Cartier Zone (Figure 5), were logged and sampled in locations where the interaction between the veins, host rock and structure was clear.

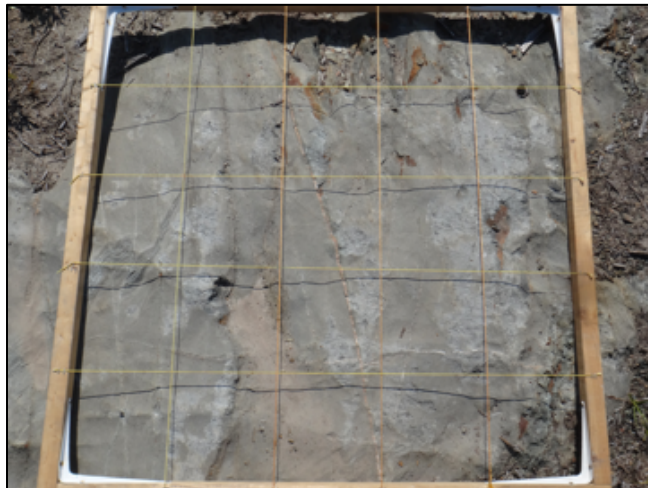


Figure 4: Example of the Grid system used to complete the detailed maps where important cross cutting relationships were observed.

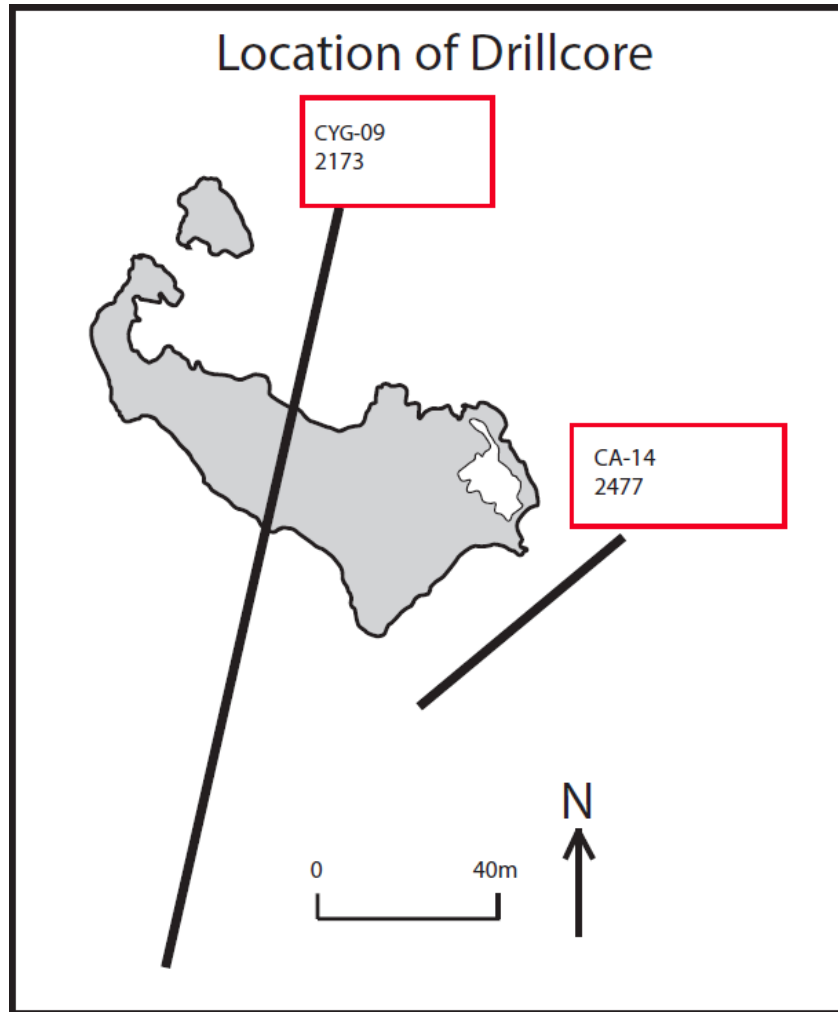


Figure 5: Location and orientation of selected drill holes projected to surface.

3.2 GEOCHEMICAL ANALYSIS OF WHOLE ROCK SAMPLES FOR GOLD CONTENT

Geochemical analysis was completed on twelve samples to examine the gold content of the vein systems. Values for element determination are semi-quantitative due to the small sample weight used (0.5g). Analyses were carried out at ACTLABS, ALS and SGS laboratories using trace element (by aqua regia-ICP, Na₂O₂ fusion-ICP, IR combustion and XRF) whole rock analysis.

Aqua regia-ICP was conducted by ALS and the prepared samples were digested with aqua regia in a graphite heating block. After cooling, the resulting solution was diluted to 12.5 ml with deionized water, mixed and analyzed by inductively coupled plasma-atomic emission spectrometry. The analytical results were corrected for inter-element spectral interference and it should be noted that data reported from an aqua regia leach should be considered as representing only the leachable portion of the particular analyte (ALS Minerals, 2009)

3.3 PETROGRAPHIC ANALYSIS

Oriented samples were taken from outcrop and drill core and thirty-two polished thin sections were prepared at Queen's University in Kingston, Ontario for optical petrographic investigation. When applicable, the thin sections were prepared perpendicular to the main foliation and parallel to the main lineation. Both transmitted and reflected light methods were used to study the samples using a polarized microscope from the Dr. Olivo petrographic laboratory. Both the vein systems and the related alteration selvage in the host rock were described in detail and compiled with the detailed vein mapping to interpret the paragenetic sequence of vein systems at Cartier Zone.

4 GEOLOGY OF CARTIER ZONE

4.1 ROCK UNITS

4.1.1 Pontiac Metasedimentary Rocks

Pontiac metasedimentary greywacke and siltstone lenses occur in succession at Cartier Zone with one lens of conglomerate occurring in the central west region of the outcrop. Greywacke is the dominant unit that and throughout the Pontiac whereas siltstone layers are more frequent in the northern and southern region of the outcrop and have a maximum thickness of 0.5m. Petrographic analysis was completed on the greywacke and siltstone lenses in conjunction with the vein systems.

4.1.1.1 *Greywacke Units*

Greywacke lenses are comprised of approximately 70% quartz, 30% feldspar with trace quantities of biotite, apatite and sulfide minerals, specifically pyrrhotite and pyrite. Quartz occurs as the primary component of the matrix and makes up 60% of the framework as grains or agglomerates (Figure 6a).

Feldspar makes up the remaining 40% of the framework and tends to have smaller grains that are more altered than the quartz framework. Fine-grained acicular biotite occurs as inclusions in the feldspar grains and between quartz grains in the matrix.

4.1.1.2 *Siltstone*

Similar to the greywacke lenses, the siltstone lenses are comprised of approximately 80% quartz with minor proportions of feldspar, biotite, and chlorite with trace amounts of ilmenite, pyrite and pyrrhotite (Figure 6d). Quartz occurs both as the framework and the matrix while the feldspar, biotite and chlorite occur in the matrix along the boundaries of the quartz framework grains. Throughout the Pontiac metasedimentary rocks bedding is observed in the siltstone lenses and is comprised of elongate 10µm

sized biotite and chlorite grains with 1-2mm sized euhedral pyrrhotite grains occurring in the biotite-rich (iron-rich) Pontiac metasedimentary rocks layer (Figure 6e).

4.1.1.3 Hydrothermal Alteration

Hydrothermal alteration in the greywacke and siltstone units is associated with two separate events. The first to occur was the silicification of the quartz rich matrix, characterized by the replacement quartz and feldspar grain boundaries. Feldspar framework grains tend to be more altered than quartz framework grains and exhibit replacement in the grain margin from the silicified quartz. Silicification of the matrix was then overprinted by the second generation of biotite that defines the S_2 foliation. The final stage of alteration was associated with alteration from vein systems in the form of weak carbonate, muscovite, chlorite and biotite replacement.

4.1.1.4 Deformation Features

The greywacke lenses typically exhibit the major S_2 foliation, which is defined by euhedral biotite grains that overprint the quartz matrix. This second generation of biotite tend to have larger 100 μ m sized irregular shaped grains that have reddish brown pleochroism (Figure 6b). The size and shape allow it to be distinguished from the primary biotite that have 10 μ m sized acicular grains. Foliation intensity varies depending on the location in outcrop. Steep isoclinal folding at the northwest region of the outcrop generated a well-defined foliation (Figure 6b), however along the limb of a fold located in the southwest region of the outcrop the foliation is weakly defined (Figure 6c).

Deformation formed amygdaloids of chlorite that overprint the quartz-feldspar greywacke in the central west region of the outcrop. Elongate hydrothermal biotite grains 350 μ m large rim the chlorite amygdaloids and constitute (30%) of the modal mineralogy of the altered host rock (Figure 6e). In the same location pyrite grains exhibit pressure shadows that cut the foliation and are therefore formed

syn-D₂ (Figure 7). The pressure shadows are defined by chlorite at the margin of the pyrite and quartz in the pressure fringes showing sinistral rotation of the pyrite grain.

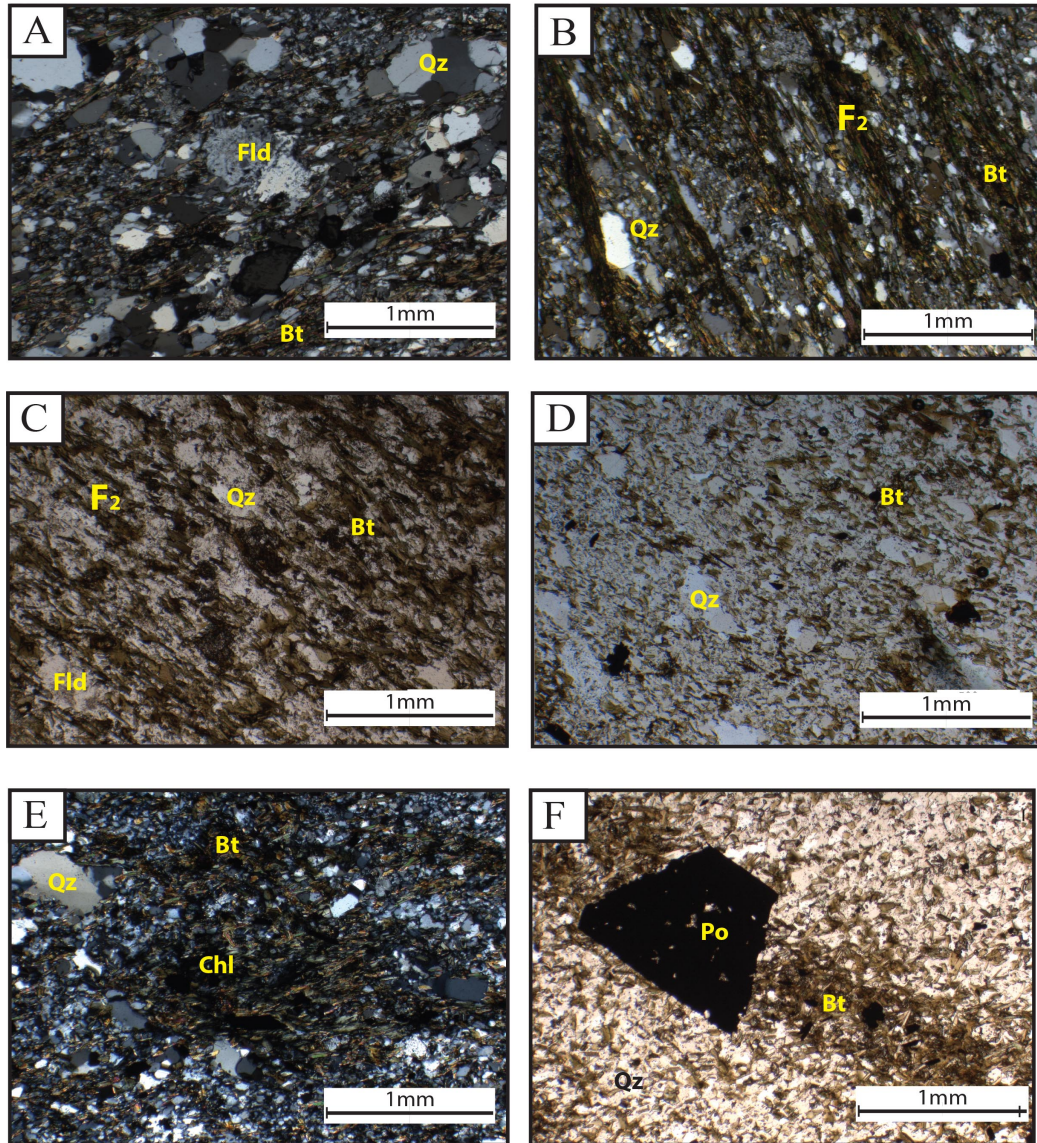


Figure 6: Photomicrographs of the Pontiac metasedimentary rocks illustrating the relevant minerals and textural relationships. A: (Sample K389761) X-Polar image of the typical Pontiac greywacke with framework grains consisting of quartz grains and conglomerates as well as altered feldspar grains. B: (Sample K389761) X-Polar image of the major S₂ foliation that is defined by elongate biotite grains. C: (Sample K389763) Plane light image of the greywacke unit where two generations of biotite are present. Hydrothermal biotite that defines the foliation replaces biotite that was originally part of the host rock. D: (Sample K389762) Plane light image showing the weak foliation defined by the oriented biotite grains. E: (Sample K389766) X-Polar image of chlorite and biotite amygdaloids that are oriented parallel to the S₂ foliation. F: (Sample K389764) Plane light image of the siltstone where large euhedral pyrrhotite grains occur in the biotite-rich (iron-rich) bedding planes.

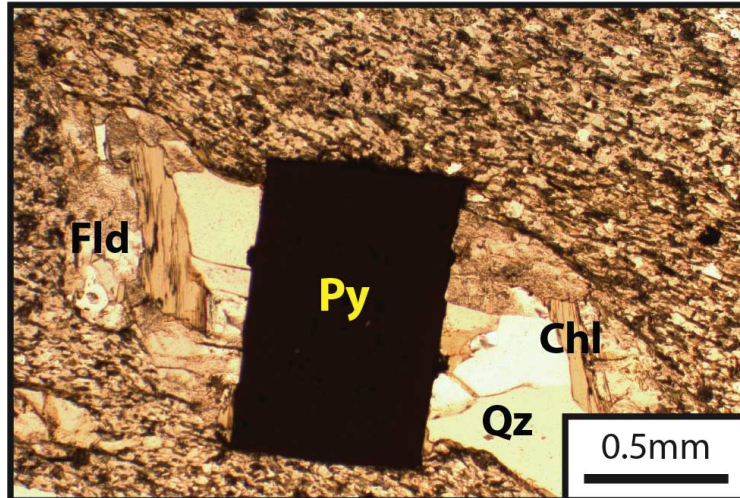


Figure 7: (Sample K389761) Plane light photomicrograph of a pyrite grain that exhibits a pressure shadow that formed syn- D_2 as it is parallel to the S_2 foliation and shows sinistral rotation.

4.1.2 Quartz Monzodiorite Intrusion

4.1.2.1 Description

The intrusion is composed of quartz monzodiorite with relative proportions between 65% feldspar, 20% quartz, 10% microcline, 5% biotite and chlorite with trace amounts of sulfides, specifically pyrite and chalcopyrite. Feldspar occurs as phenocrysts that exhibit albite and microcline twinning (Figure 6a) while fine-grained quartz makes up the groundmass. The albite phenocrysts range in size from 0.5-2 and tend to be replaced at the crystal margins by the quartz groundmass.

The modal abundance of albite and quartz is higher than what was described by Neumayr et al. (2000).

Therefore the rock composition is within the quartz monzodiorite range. This correlates with results from Gunning and Ambrose (1940) with modal compositions of the intrusion at 50% albite (An₃), 20% quartz and 10-15% microcline.

4.1.2.2 Hydrothermal Alteration

Depending on the location within the intrusion there are different degrees of alteration. In the central region of the outcrop the intrusion remains relatively unaltered (Figure 8a) Closer to the contact with the Pontiac metasedimentary rock the quartz monzodiorite intrusion is altered by pervasive silicification of the matrix that replaces feldspar phenocryst boundaries. This results in the proportion of quartz increasing up to 50% of the modal abundance (Figure 8b). At the contact with the Pontiac metasedimentary rock the feldspar phenocrysts are either partially or completely replaced by pyritization and biotite/chlorite replacement (Figure 8c). Muscovite, biotite and chlorite stringers also crosscut the quartz monzodiorite intrusion. The stringers do not appear to be associated with the characterized vein systems and generate minimal alteration of the host rock. Throughout the intrusion weak alteration in the form carbonate, biotite, chlorite and muscovite replace the quartz-rich groundmass and the feldspar phenocryst margins (Figure 8d).

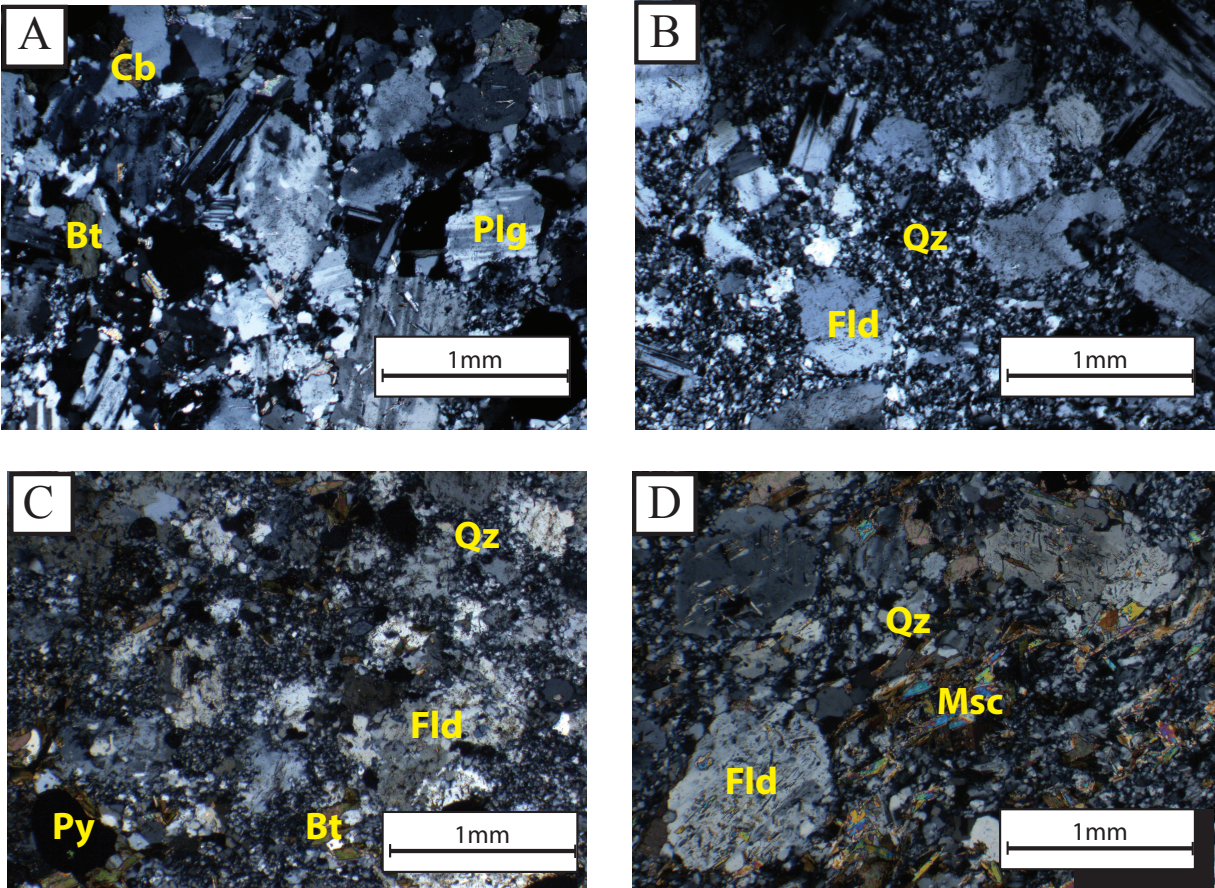


Figure 8: Photomicrographs of the quartz monzodiorite intrusion illustrating the relevant minerals and textural relationships. A: (Sample K389810) X-polar image of the most unaltered section of the intrusion with plagioclase phenocrysts and quartz groundmass showing minor carbonate replacement. B: (Sample K389815) X-Polar image showing silicification of the groundmass and replacement of the phenocryst margins. C: (Sample K389769) X-Polar image of alteration at the contact between the intrusion and the Pontiac metasedimentary rocks in the form of silicification, pyritization, biotite and chlorite alteration. D: (Sample K389776) X-Polar image showing muscovite and carbonate replacement of the groundmass.

4.2 DEFORMATION

As discussed by Gunning and Ambrose (1940) the outcrop is located at intersection of a F_1 and major F_2 fold hinge. Since Cartier Zone is in the hinge of a major F_2 fold, it is possible to clearly establish relationships between the D_1 and D_2 event. Structural mapping was completed in 2014 (Figure 9) and

correlates with the structural maps generated by Gunning and Ambrose (1940) and Neumayr et al. (2000).

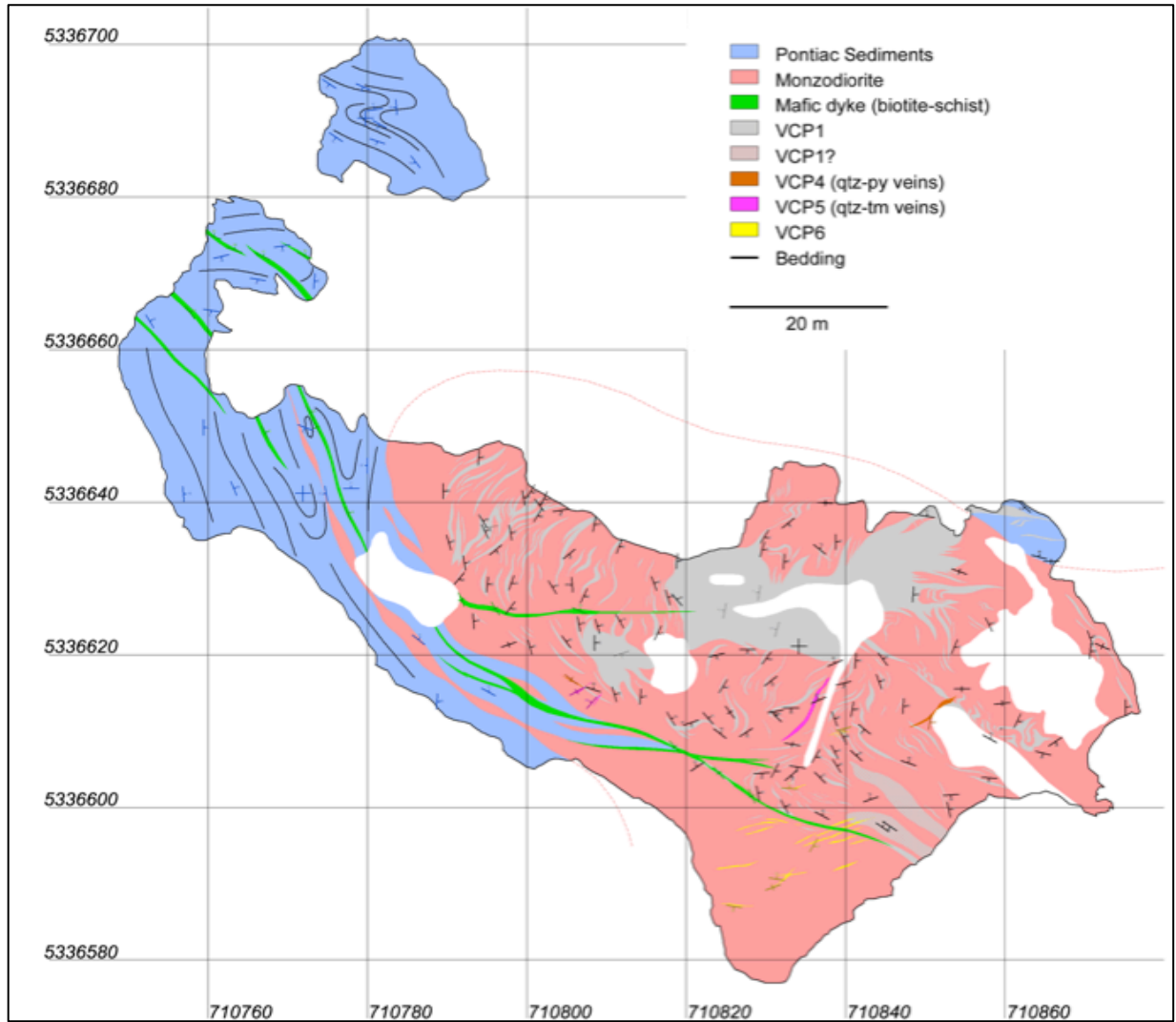


Figure 9: Geologic map of Cartier Zone (compiled by S. Perrouty, personal communication).

The D_1 event was characterized in the Pontiac metasedimentary rocks by isoclinal folding, sub-parallel bedding fabrics and vein systems. After the D_1 event, the quartz monzodiorite intrusion and mafic dykes were emplaced and the D_2 event occurred. The D_2 event was characterized by the main foliation in the Pontiac metasedimentary rocks and the intrusion, folding, and by cross cutting relationships between

vein systems. The D_3 event was distinguished from the D_2 event by open folding of F_2 (Figure 10) and the orientation of vein systems that were located in the Pontiac metasedimentary rocks and the intrusion.

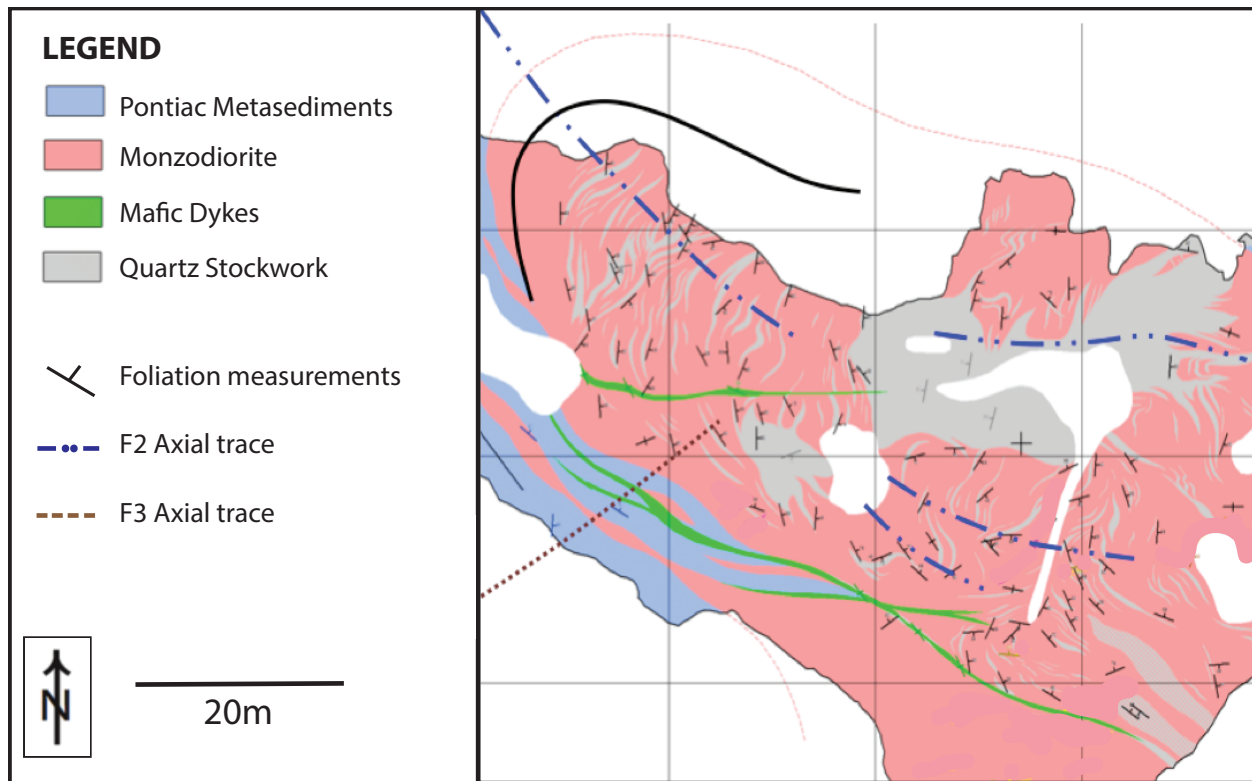


Figure 10: Incorporating the large-scale structural features onto the Geologic Map at Cartier Zone (compiled by S. Perrouty, personal communication).

5 CHARACTERIZATION OF THE VEIN SYSTEMS

During this study, eleven vein systems were characterized at Cartier Zone, three of which were observed in both rock types. Each of the vein systems were identified using orientation, composition of the vein and alteration selvage and cross cutting relationships. Vein systems were named systematically from A to K and put into a chronological sequence based on cross cutting relationships with bedding, foliation and other vein systems.

5.1 DETAILED MAPS

Detailed maps were completed in four locations (Figure 11) where cross cutting relationships were clear. Two were completed in the Pontiac metasedimentary rocks and the remaining two were completed in the quartz monzodiorite intrusion.

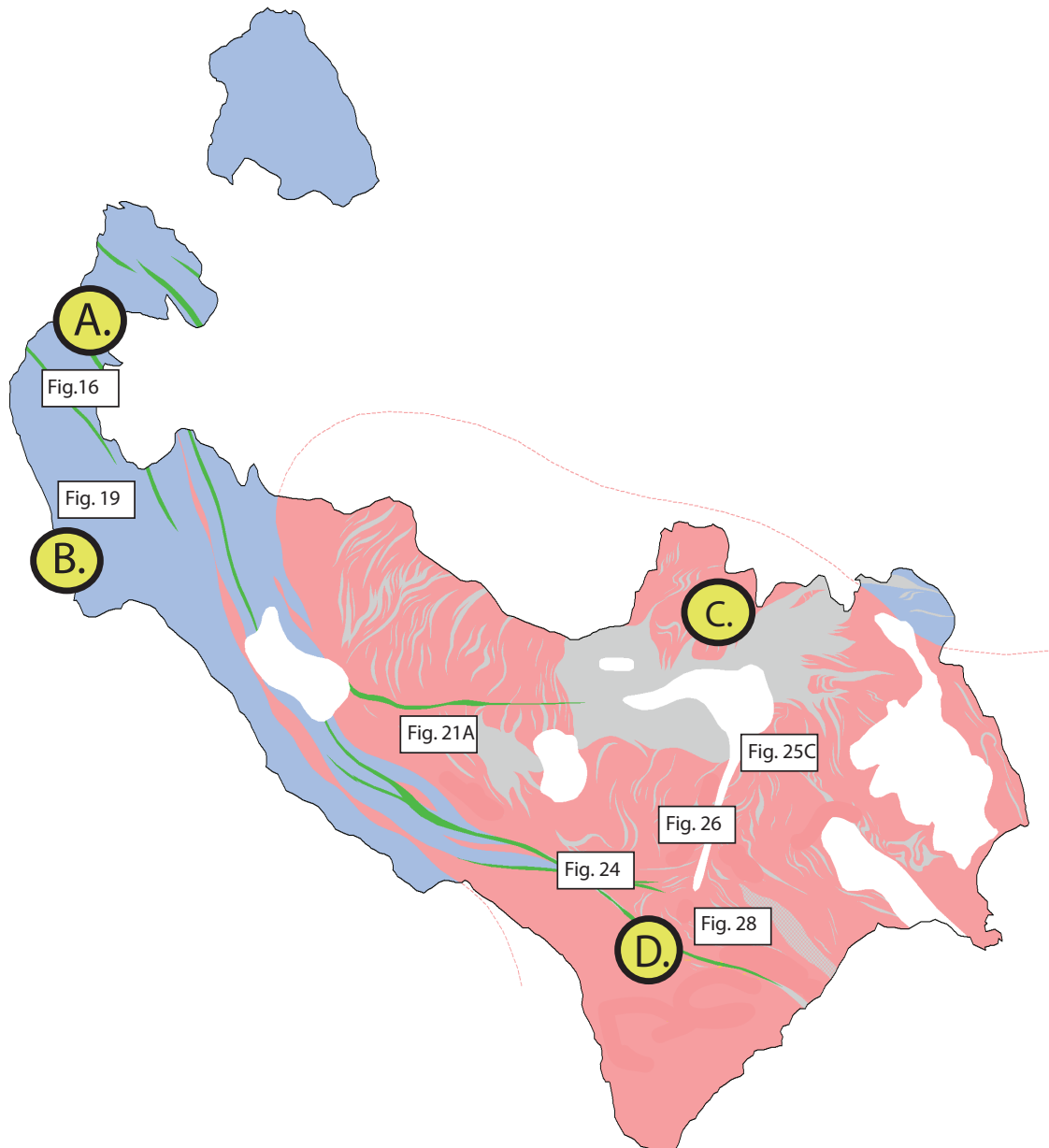


Figure 11: Location of the four detailed maps and figures illustrating key vein relationships. Geological map compiled by S. Perrouty (personal communication).

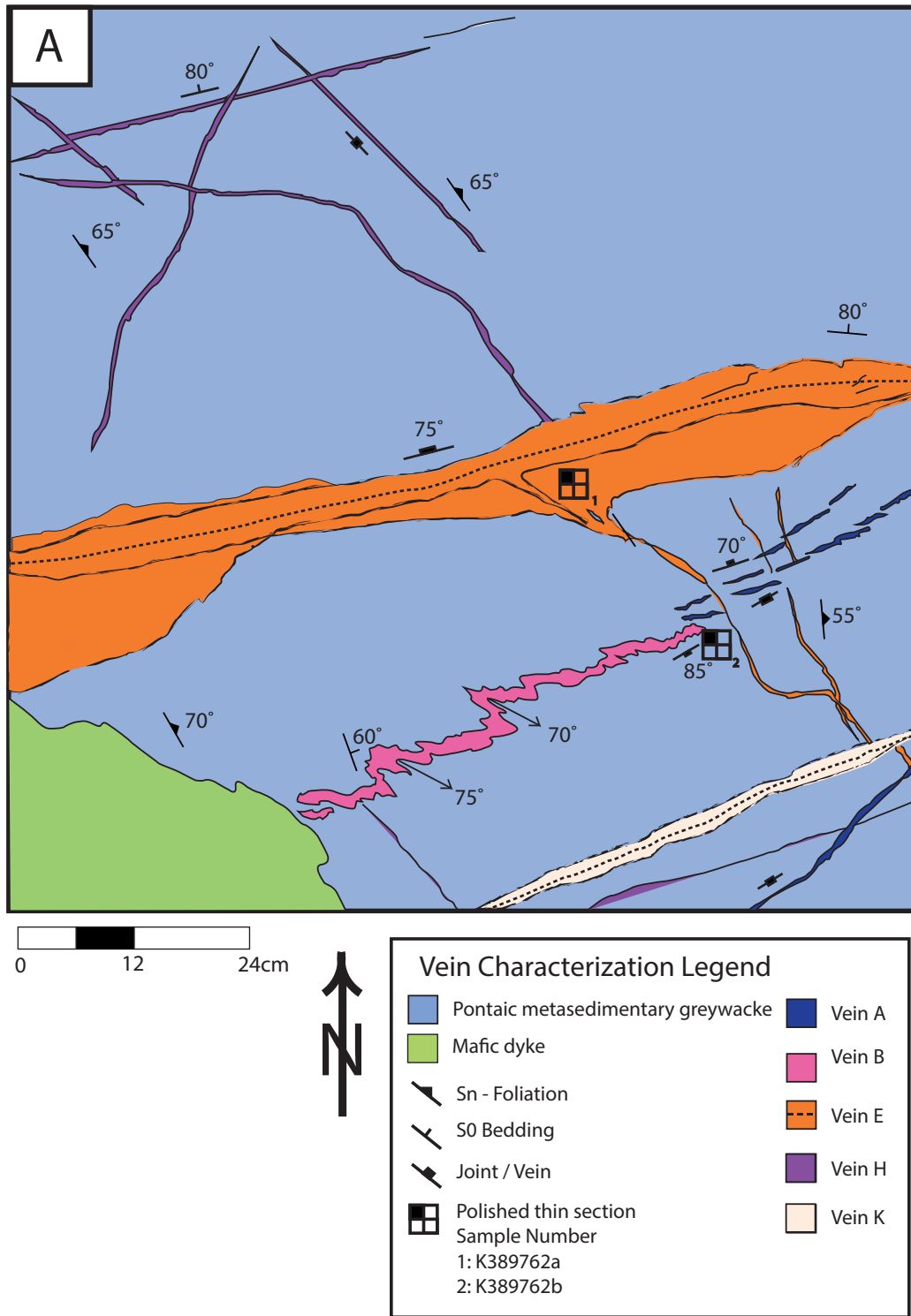


Figure 12: Detailed map A illustrates cross cutting relationships amongst the vein systems that formed pre-D₂ and the size of the alteration selvage generated by the 1mm sized E veinlet. The foliation is more intense in this location so cross cutting relationships with the major S₂ foliation assisted in determining vein chronology.

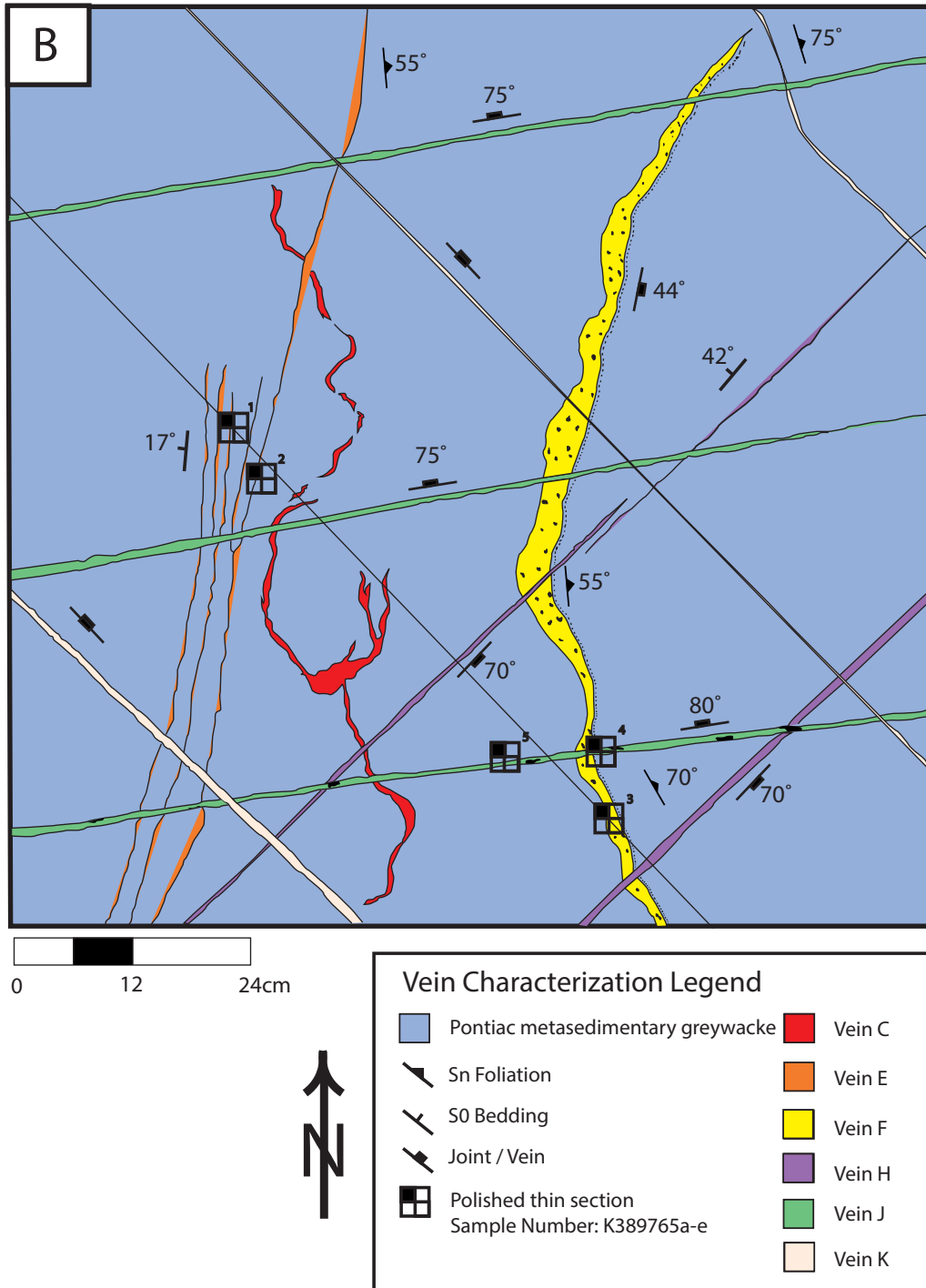


Figure 13: Detailed map B illustrates the cross cutting relationships amongst six of the eight vein systems that occur in the Pontiac metasedimentary rocks. Vein chronology was determined by relationships to foliation and bedding for the systems occurring Pre-D₂ and more on cross cutting relationships with other veins for vein systems that formed Post-D₂.

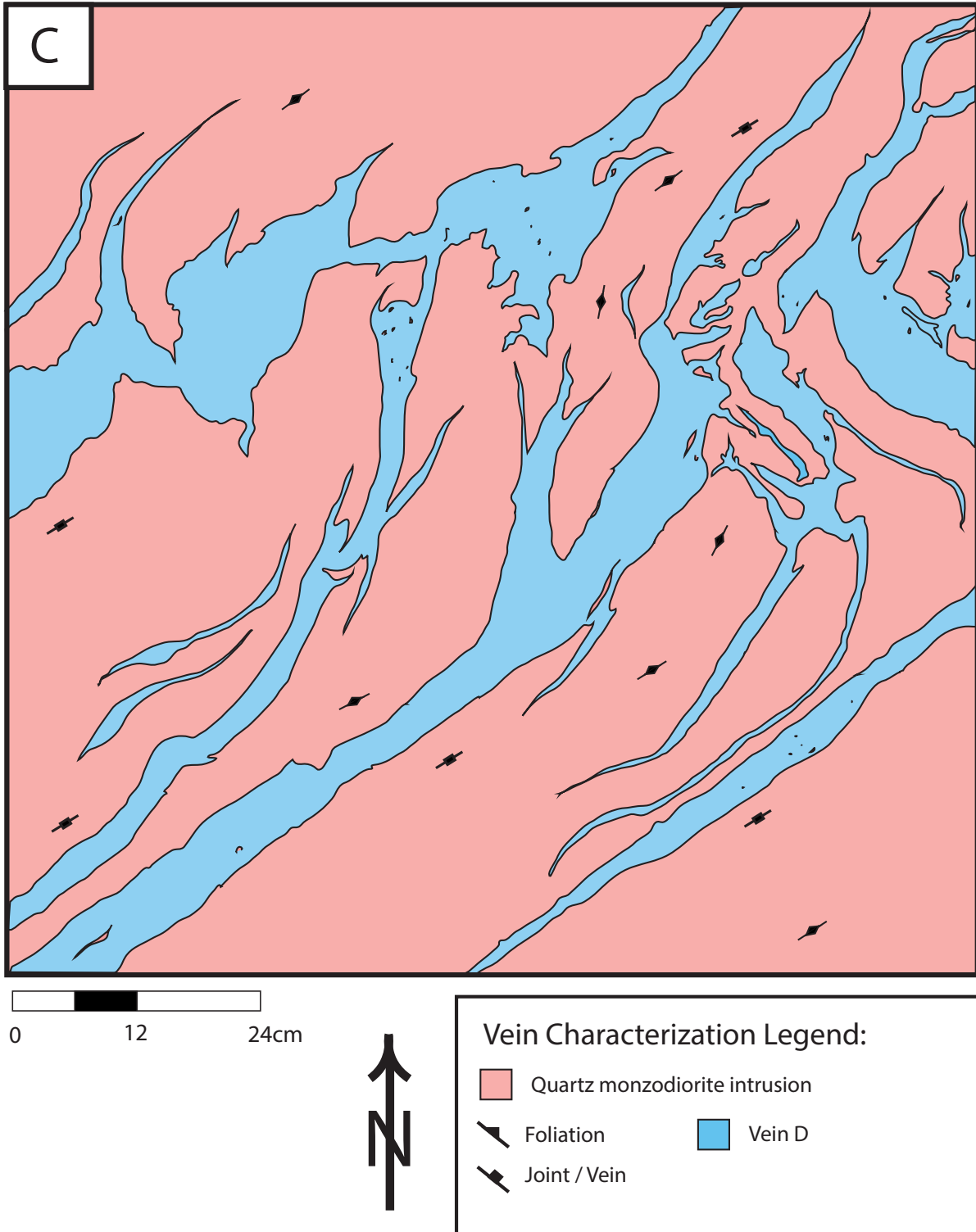


Figure 14: Detailed map C examines the Vein D system exclusively to show how the deformation of the veins form parallel to S_2 foliation that occurred in the quartz monzodiorite intrusion.

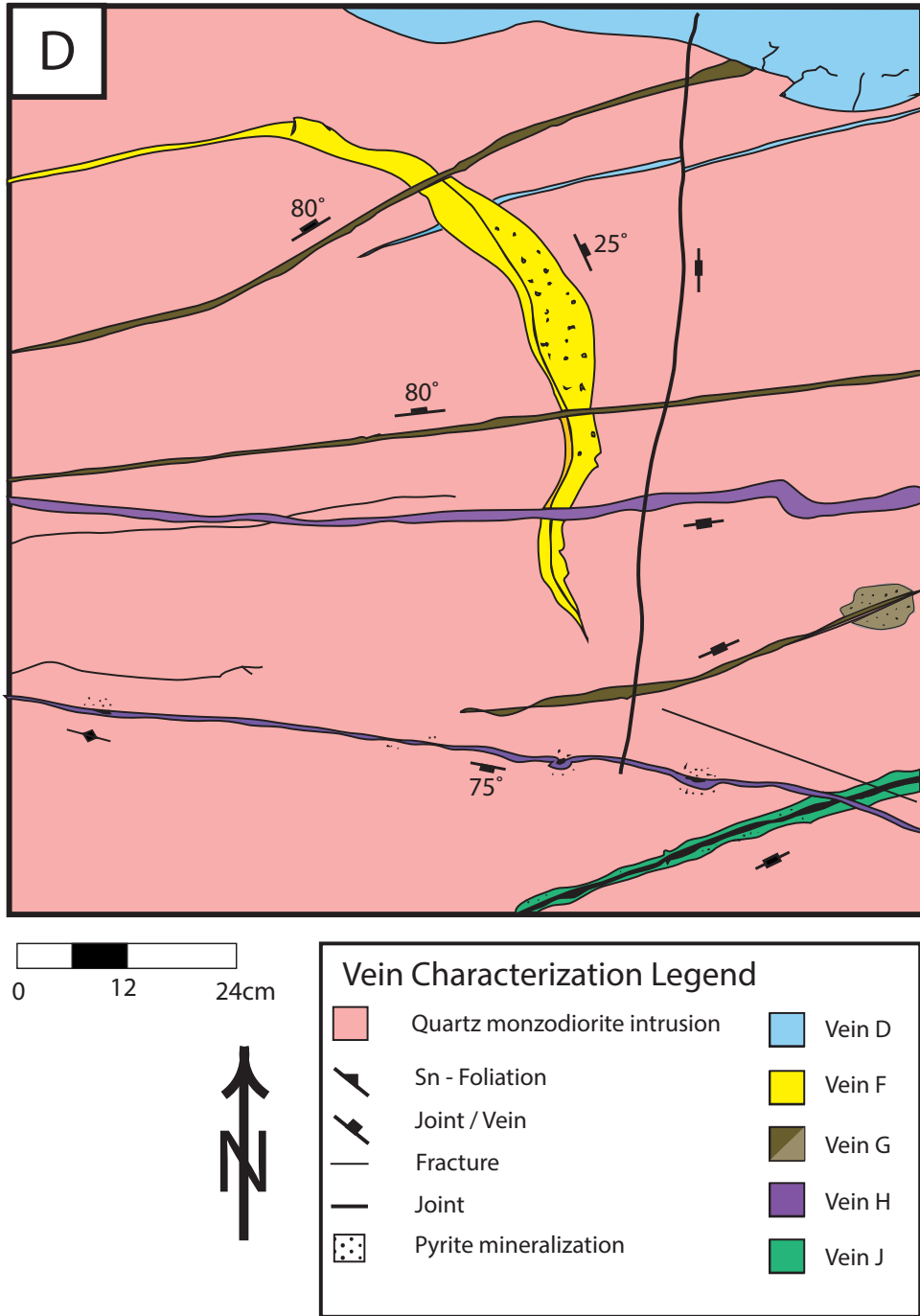


Figure 15: Detailed map D illustrates the interaction between five of the eight vein systems that occur in the quartz monzodiorite intrusion. Surface weathering generated vuggy cavities in the Vein H systems and an oxidized selvage surrounding the Vein J system.

5.2 VEIN A

5.2.1 Structural Controls and Geometry

Vein A system is composed of two subtypes and is only observed in the Pontiac metasedimentary rocks. Depending on the location of the vein systems, the style of deformation is different. The common feature between vein subtypes is that they were deformed by the major D₂ event and therefore formed pre-D₂. Veins that occurred near the hinge of the major fold, as seen in Detailed map A (Figure 12), were offset and tightly folded by the D₂ event. Along the limbs of the isoclinal folding, the veins were transposed along S₂ and oriented 280°/90 (Figure 16).

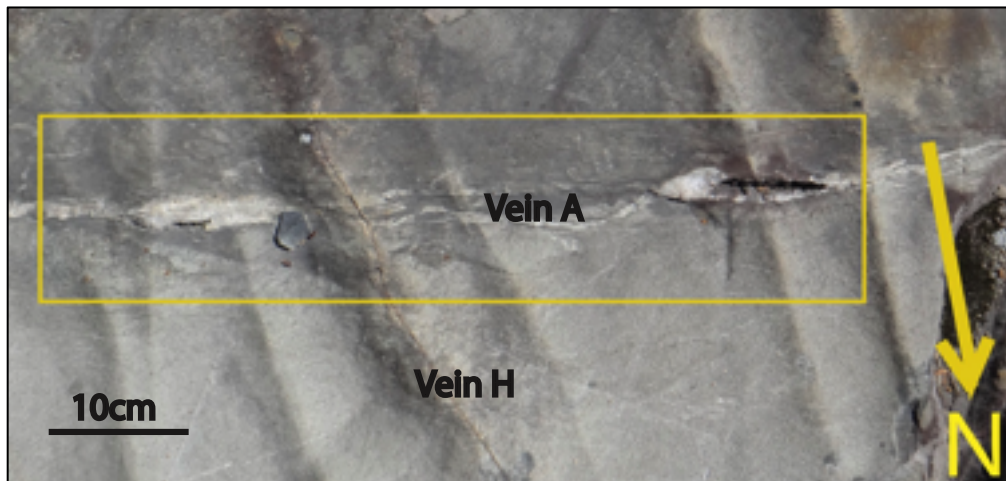


Figure 16: Vein A transposed along S₂ crosscut by Vein H.

5.2.2 Mineralogy

The first vein subtype was located in the central west region of the outcrop and are in sharp contact with the Pontiac metasedimentary rock. It is composed of quartz (95%) and feldspar (5%) with trace chlorite and biotite. The accessory minerals are localized in the vein margin and fill fractures between the quartz crystals (Figure 17a), however, no selvage alteration is associated with this vein subtype.

The second vein subtype was located in the northwest corner of the outcrop where the vein are in sharp contact with the Pontiac Metasedimentary rock. It is composed of quartz (85%) and feldspar (15%) with trace biotite. The quartz grains are up to 2mm large and become finer grained closer to the margin of the vein while feldspar is localized along the vein margin (Figure 17b). Again, no alteration selvage is present with this vein subtype.

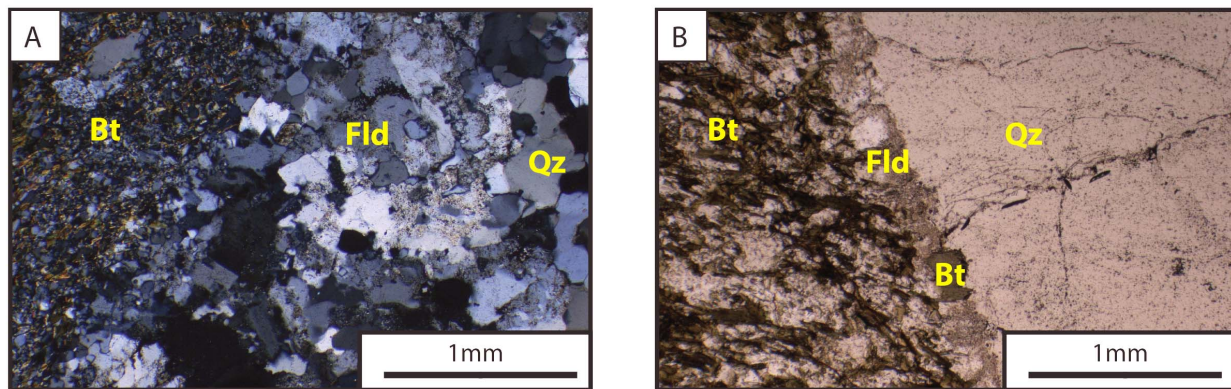


Figure 17: Photomicrographs of the Vein A system illustrating the relevant minerals and textural relationships. A. (Sample K389763) X-Polar image of the first subtype showing the sharp contact between the vein and Pontiac metasedimentary host rock where feldspar crystalizes in the vein margin and replaces the quartz grains. B. (Sample K389762) Plane light image of the second subtype showing the contact between the vein and host rock where fine grained feldspar and biotite form in the vein margin/selvage.

5.3 VEIN B

5.3.1 Structural Controls and Geometry

Similar to Vein A, this vein system occurs in the Pontiac metasedimentary rocks and only appears in the northwest region of the outcrop. The Vein B system is sub parallel to folded bedding where the axial trace correlates with the general orientation of the S_2 foliation as seen in detailed map A (Figure 12). Since the vein is deformed by the D_2 event it was interpreted to have formed pre- D_2 .

5.3.2 Mineralogy

The Vein B system is composed of quartz (90%) with minor amounts of feldspar (5%) and iron-rich chlorite (5%) that concentrate in the vein margin (Figure 18). Fractures between the crystallized quartz grains are filled with feldspar, whereas the Fe-chlorite forms fibrous patches overprinting the quartz and feldspar. Vein B are in sharp contact with the host rock with no evidence of selvage alteration associated with the vein system.

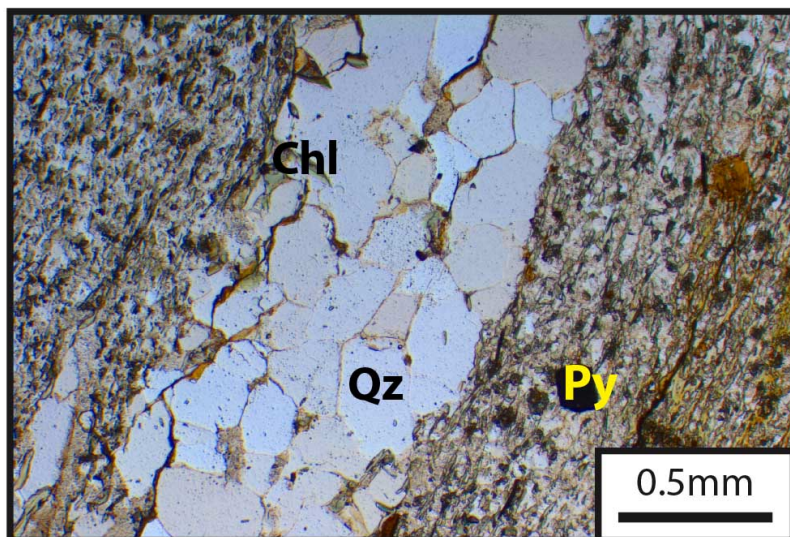


Figure 18: (Sample K389762) Plane light photomicrograph of the Vein B system illustrating the sharp contact between Vein B and the Pontiac metasedimentary host rock where Fe-chlorite forms in the vein margin.

5.4 VEIN C

5.4.1 Structural Controls and Geometry

The Vein C system is located in the Pontiac metasedimentary rocks and is the last of the vein systems to form pre-D₂. Vein C is shallow dipping and cuts bedding (Figure 19). As illustrated in Detailed map B, the vein is deformed by the D₂ event and was sheared along the S₂ plane (Figure 13).

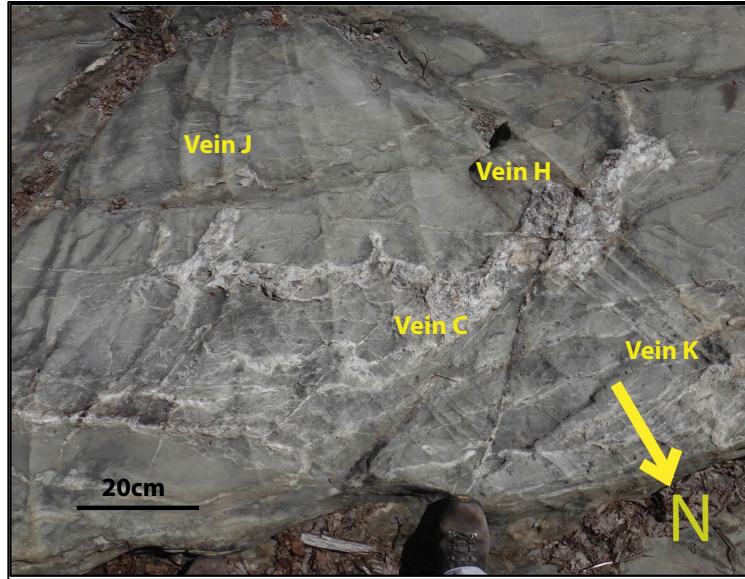


Figure 19: Vein C with shallow dip was deformed by the D_2 event.

5.4.2 Mineralogy and Selvage Alteration

The Vein C system is composed of quartz (60%), feldspar (30%) and chlorite (10%) with trace amounts of ilmenite, pyrite, and chalcopyrite. Feldspar fills corroded zones in quartz crystals in the vein margins and is overprinted by the chlorite (Figure 20a).

In the wall-rock within 1cm of the vein, fine-grained quartz replaced the rock matrix but did not replace biotite (Figure 20b). The biotite grains that occur in the selvage are fine grained, elongate and randomly oriented similar in size, shape and orientation to the biotite found further into the unaltered host rock.

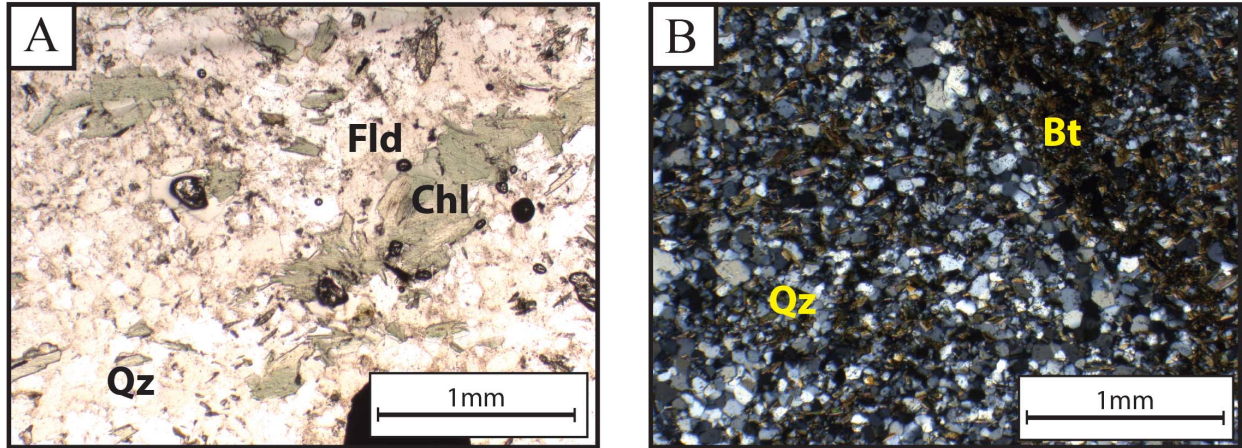


Figure 20: Photomicrographs of the Vein C system illustrating the relevant minerals and textural relationships. A: (Sample K389764) Plane light image of chlorite overprinting feldspar in the vein margin. B: (Sample K389764) X-polar image of the quartz rich alteration selvage where biotite from the original host rock is preserved in the selvage.

5.5 VEIN D

5.5.1 Structural Controls and Geometry

Vein D is the first vein system to form in the quartz monzodiorite intrusion. Vein D forms as massive veins that are up to 2m thick, extend 20m in length and exhibit echelon folding throughout the intrusion as seen in Detailed map C (Figure 14). The Vein D systems is parallel to the S_2 foliation which is folded by the F_3 folds, and is therefore interpreted to have been deformed during the D_3 event and formed either pre- to syn- D_2 .

5.5.2 Mineralogy and Selvage Alteration

The Vein D system is composed of quartz (90%) that is up to 2mm in size and shows evidence of strain through sutured contact between grains (Figure 21b). Carbonate (10%) occurs in the margin of the vein with trace amounts of carbonate, chlorite, and muscovite occur between fractures in the quartz grains. Due to cross cutting relationships the fracture filling minerals are interpreted to be associated with later alteration (Figure 21c).

Contact between the Vein D and quartz monzodiorite intrusion is sharp (Figure 21d) and carbonate alteration forms a 1-2mm selvage (Figure 21a). Based on optical analysis and comparisons between size, colour and habit, pervasive carbonate alteration that replaces the feldspar phenocrysts in the intrusion is interpreted to be associated with the Vein D system.

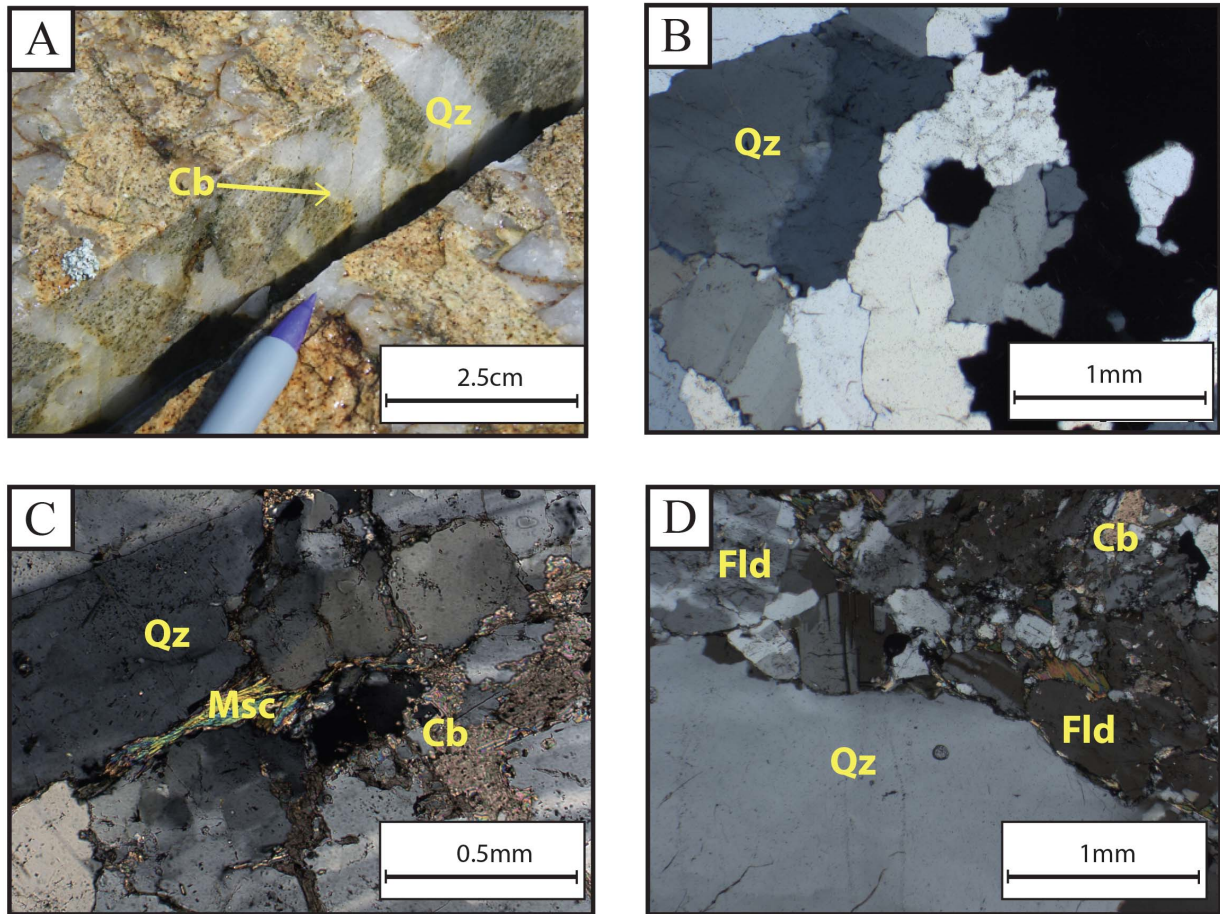


Figure 21: Photomicrographs and field observations of the Vein D system illustrating the relevant minerals and textural relationships. A: Image from the outcrop showing 1mm carbonate alteration in the selvage. B: (Sample K389810) X-Polar image of the sutured contact between quartz grains. C: (Sample K389810) X-Polar image of carbonate and muscovite alteration that replaces quartz at the grain margins. D: (Sample K389810) X-polar image of the sharp contact between the vein and host rock.

5.6 VEIN E

5.6.1 Structural Controls and Geometry

The Vein E system is comprised of thin 1mm sized veinlets that occur exclusively in the Pontiac metasedimentary rock. They are most abundant close to the location of Detailed map A and form in composite sets oriented $050^{\circ}/90$ and $090^{\circ}/90$ (Figure 12). The Vein D system crosscuts the S_2 fabric and therefore formed post- D_2 .

5.6.2 Mineralogy and Selvage Alteration

The Vein E system makes sharp contact with the surrounding Pontiac metasedimentary rock and is composed entirely of plagioclase exhibiting carlsbad twinning (Figure 22). The 0.5mm-0.85mm sized plagioclase crystals are elongate and grow from the margin of the vein towards the center.

Selvage alteration formed up to 5cm on either side of the veinlet. The hydrothermal alteration recrystallized the original quartz rich greywacke into a very fine-grained quartz, feldspar, and muscovite matrix with a modal abundance of 80% quartz-feldspar and 20% muscovite respectively. Proximal alteration is dominated by quartz and feldspar while the proportion of muscovite increases further into the selvage, filling the margin between the silicified quartz grains.

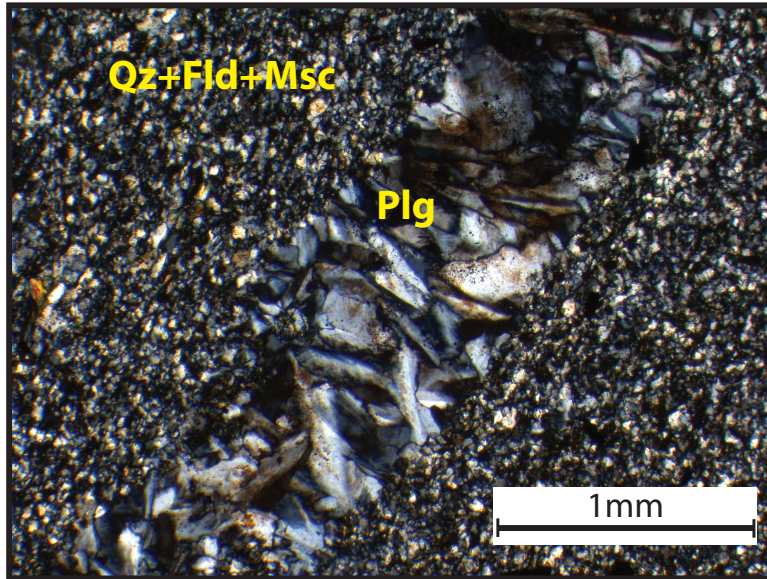


Figure 22: (Sample K389762) X-polar photomicrograph of the Vein E system showing the sharp contact between the vein which exhibits inter-fingering of feldspar grains and the host rock that was replaced by quartz, feldspar and muscovite in the alteration selvage.

5.7 VEIN F

5.7.1 Structural Controls and Geometry

The Vein F system is the first to appear in both rock types. The veins tend to be openly folded, following a general orientation of $010^{\circ}/45$ in the Pontiac metasedimentary rock and $135^{\circ}/45$ in the intrusion. The vein crosscuts the main S_2 foliation in both rock types and therefore formed post- D_2 .

5.7.2 Mineralogy and Selvage Alteration

In the quartz monzodiorite intrusion Vein F is composed of quartz (75%) with sutured contact between crystals and (25%) carbonate with trace amount of chlorite, pyrite and chalcopyrite forming in fractures between the quartz crystals. Carbonate forms in patches, cutting through the quartz crystals in the vein (Figure 23b) and is associated with chlorite, pyrite and chalcopyrite. Vein F appears to have experienced more strain than Vein D as the sutured contact between the grains is more prominent (Figure 23a).

Similar proportions of quartz (60%) and carbonate (40%) were found in the Pontiac metasedimentary rocks. Quartz crystals exhibit minor strain through undulatory extinction and carbonate concentrates in the vein margin preferentially on one side and replaces biotite from the host rock at the contact (Figure 23c). The F vein system are in sharp contact with the host rock in both rock types and no selvage alteration is present.

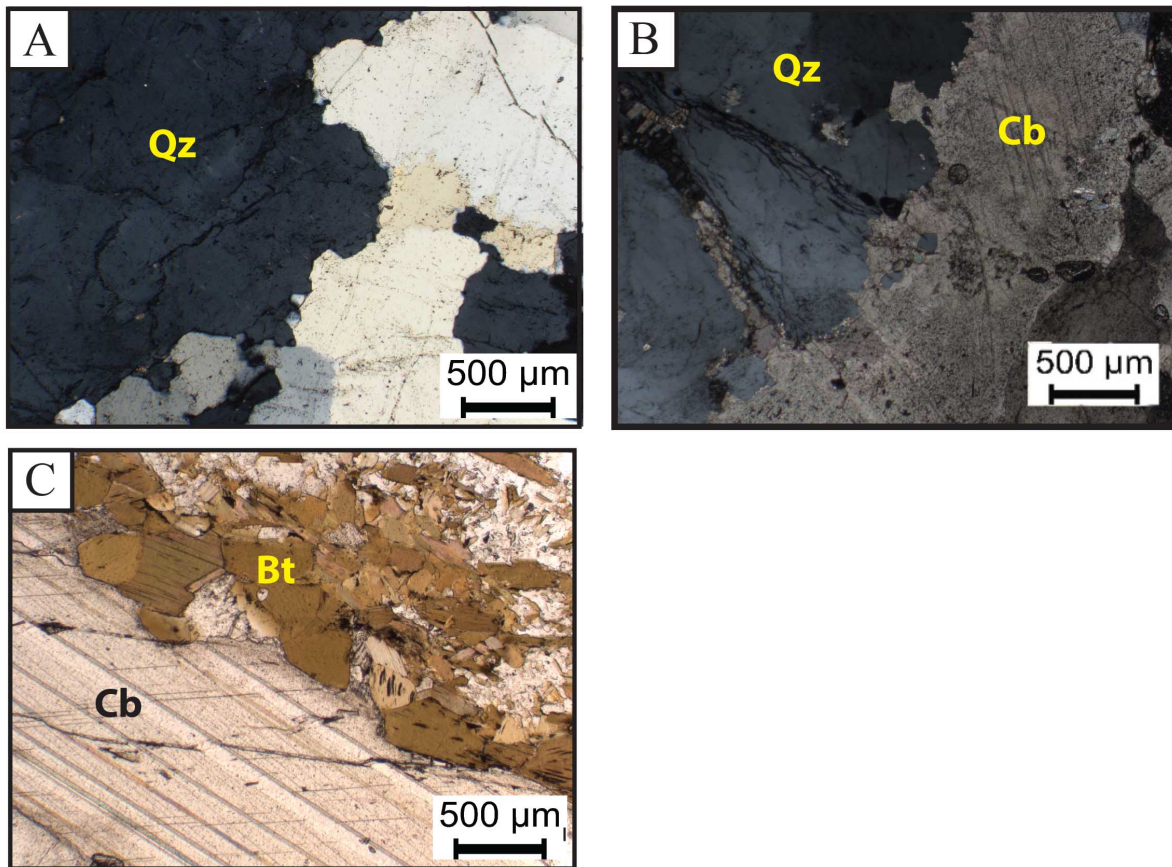


Figure 23: Photomicrographs of the Vein F system illustrating the relevant minerals and textural relationships. A: (Sample K389855) X-Polar image of the sutured texture between quartz grains in the intrusion. B: (Sample K389855) X-polar image of carbonate replacing the quartz crystals in the intrusion. C: (Sample K389860) Plane light image of the vein margin where carbonate shows minor replacement of biotite in the Pontiac metasedimentary host rock.

5.8 VEIN G

5.8.1 Structural Controls and Geometry

The Vein G system occurs in the intrusion and forms two composite vein sets formed at $280^{\circ}/75$ and $260^{\circ}/90$ (Figure 24). Relative timing of the vein system was determined through cross cutting relationships with other vein systems. Vein G was seen to crosscut Vein F and therefore the vein system must have formed Post- D_2 (Figure 15).

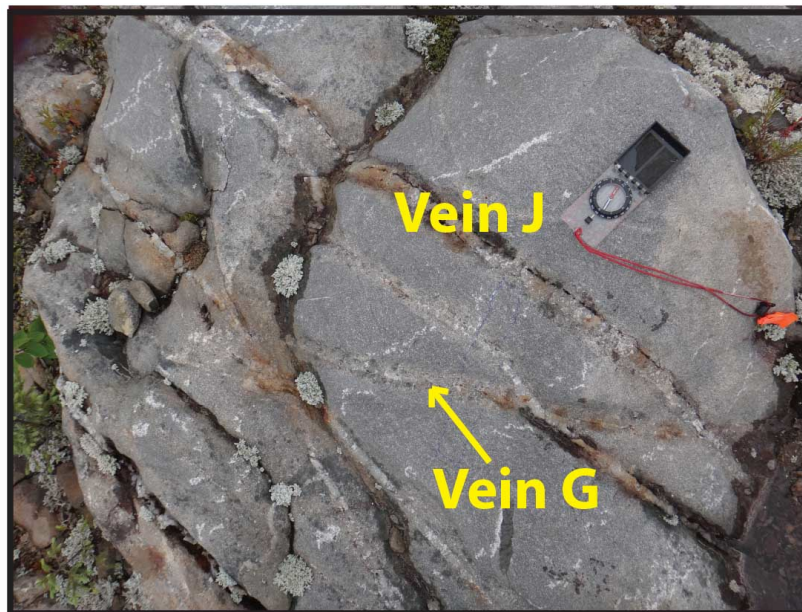


Figure 24: Image taken from the southwest region of the outcrop where the composite Vein G system was most prevalent. Oxidation occurs in the vein margin while a 3mm thick bleached alteration halo forms in the selvage. Vein G is cross cut by the Vein J system.

5.8.2 Mineralogy and Selvage Alteration

Samples of the Vein G system were not collected from outcrop and were not included in the selected samples for petrographic analysis from the drill core. From observations at outcrop, the vein is composed primarily of crystalline quartz. There are small millimeter sized cavities in the vein that are oxidized and are interpreted to have formed from replacement of sulfides.

Selvage alteration extended up to 3mm on either side of the vein and is composed of biotite and chlorite near vein margin with bleached light pink alteration further out. Since petrographic analysis was not completed for this vein system the mineralogical components of the pink alteration are unknown and the modal abundance of the vein system was not determined.

5.9 VEIN H

5.9.1 Structural Controls and Geometry

Vein H is the second vein system to be observed in both rock types. The orientation of veins in the intrusion varies along the outcrop from $080^{\circ}/90$ to $110^{\circ}/90$, whereas in the sediments the orientation is consistent at $070^{\circ}/70$. Vein H cross cuts both the Vein F and Vein G systems (Figure 15) and was therefore identified as post- D_2 . The gradual change in vein orientation in the intrusion corresponds with the open folding of S_2 from the D_3 event, therefore the vein system was identified as pre- D_3 and generates an upper boundary for a vein systems in the intrusion that formed Post- D_2 . Due to competency contrast between the two rock types, vein thickness varies from the sediments and porphyry between 1mm-1cm and spacing varies from 0.5m to 10m respectively.

5.9.2 Mineralogy and Selvage Alteration

Due to selected sampling Vein H was only characterized in the intrusion and is comprised of quartz (85%) and pyrite (15%). At surface the pyrite aggregates are weathered forming a boxwork texture (Figure 25a). Vein H has the highest proportion of pyrite compared to the other vein systems at the Cartier Zone and exhibits the highest degree of strain in the quartz as the crystals are embayed and range in size from 0.01- 2mm (Figure 25b). Selvage alteration occurs in the form of silicified quartz and replaces the feldspar phenocrysts with quartz 0.1mm large (Figure 25c).

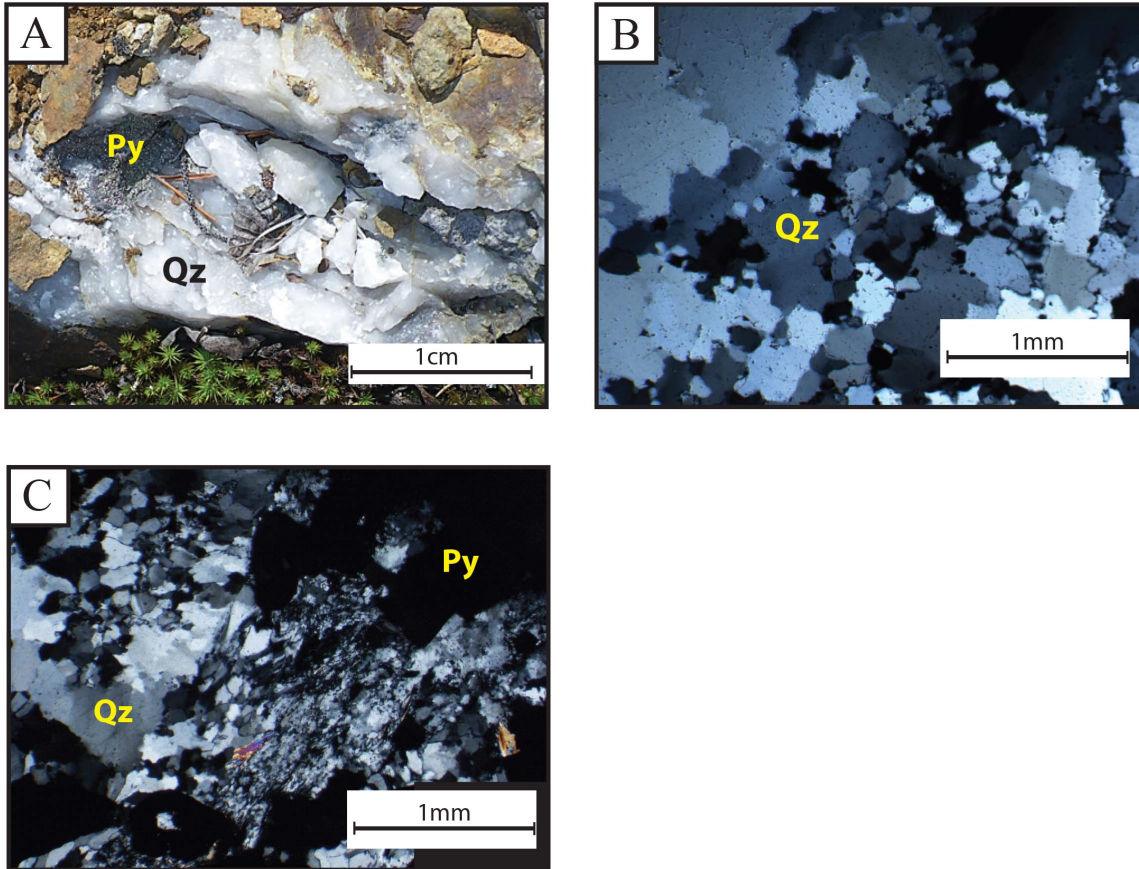


Figure 25: Photomicrographs and field observations of the Vein H system illustrating the relevant minerals and textural relationships. A: Image from outcrop showing pyrite weathering that formed boxwork texture. B: (Sample K389774) X-polar image of embayed quartz grains in the vein. C: (Sample K389774) X-Polar image of fine-grained quartz that occurs with pyrite in the vein margin.

5.10 VEIN I

5.10.1 Structural Controls and Geometry

The Vein I system was observed in the intrusion as one vein set 3cm thick (Figure 26). Vein I crosscut the Vein H system and the open folding of the vein suggested that it underwent deformation and was therefore classified as post-D₂ to pre-D₃.

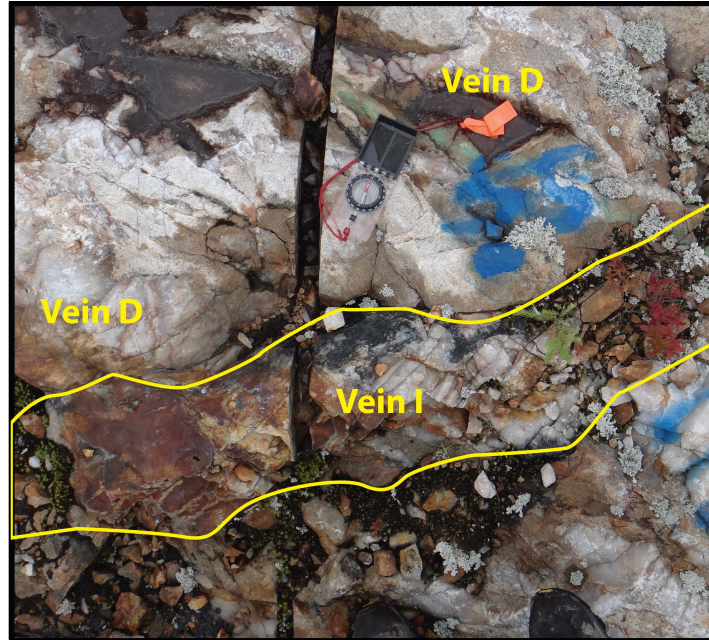


Figure 26: Vein I was observed in the central region of the quartz monzodiorite intrusion cross cutting Vein D where tourmaline is observed at the vein margin.

5.10.2 Mineralogy and Selvage Alteration

The Vein I system is composed of quartz (60%) and tourmaline (40%). The tourmaline was unevenly distributed in the vein and concentrated in zones. Quartz and tourmaline formed in the same time frame as the tourmaline forms inclusions in the quartz whereas in other regions tourmaline overprints quartz grains (Figure 27). The contact between the vein and the host rock is gradational with tourmaline replacing plagioclase phenocrysts up to 1cm into the host rock.

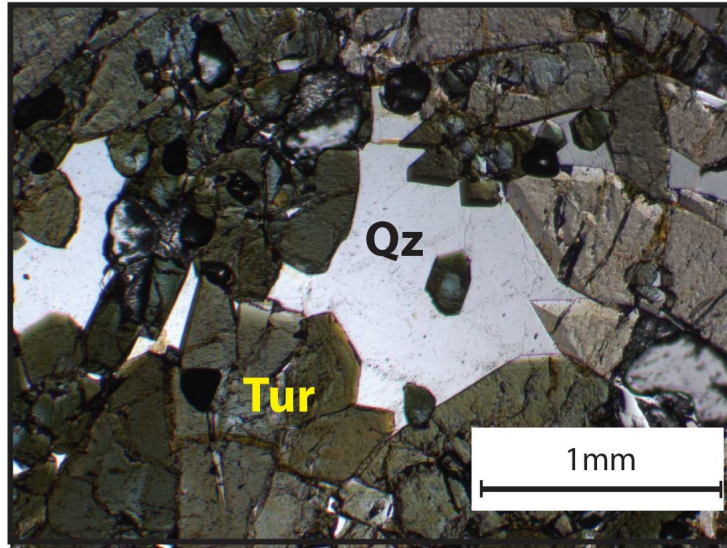


Figure 27: (Sample K389771) X-polar photomicrograph of the Vein I system illustrating the relationship between the quartz and tourmaline in the vein. Both quartz and tourmaline formed in the same time frame since tourmaline forms as inclusions in the quartz while other tourmaline grains make sharp contact with the quartz.

5.11 VEIN J

5.11.1 Structural Controls and Geometry

Vein J is the last system to occur in both rock types. The vein system have a consistent orientation through the Cartier Zone and forms composite sets oriented $275^{\circ}/90$ and $300^{\circ}/65$, crosscutting all previous vein systems found in the porphyry (Figure 28). Consistent orientation within both rock types suggests that the vein system occurred post- D_3 . The veins are thicker in the intrusion (2cm) compared to the Pontiac metasedimentary rocks (5mm), caused by competency contrast between the rock types.



Figure 28: Image of Vein J in the intrusion showing the composite sets oriented $275^{\circ}/90$ and $300^{\circ}/65$ cross cutting the Vein G system. Surficial weathering formed the oxidized vuggy cavities.

5.11.2 Mineralogy and Selvage Alteration

Due to selected sampling Vein J was only characterized in the intrusion. The veins are in sharp contact with the quartz monzodiorite intrusion and are composed of quartz (90%) with minor proportions of carbonate (5%) (Figure 29a). Carbonate occurs at the boundaries of the quartz crystals. Albite (5%) also occurs in the vein but is interpreted to have been part of the original quartz monzodiorite intrusion. Evidence of strain is observed through sutured contact between quartz crystals.

Selvage alteration associated with Vein J can extend up to 30cm as seen in drillcore. Alteration of the host rock is comprised of carbonate, biotite, chlorite and muscovite (Figure 29b). Carbonate alteration is zoned varying in proportion from 5% within 2cm of the vein to 1% further out. Biotite and chlorite have the same relative proportion throughout the sample whereas muscovite replacement is zoned with an increase in concentration from 1% to 5% away from the vein margin.

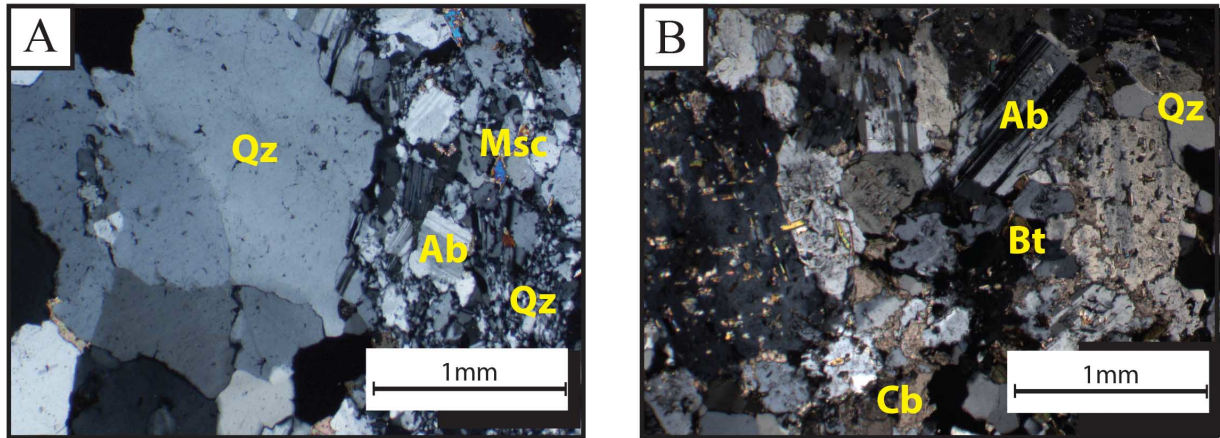


Figure 29: Photomicrographs of the Vein J system illustrating the relevant minerals and textural relationships. A: (Sample K389815) X-polar image of the sharp contact between the quartz rich vein and the quartz monzodiorite host rock. B: (Sample K389776) X-polar image of alteration attributed to the vein J system where carbonate and biotite replacement of the plagioclase phenocrysts.

5.12 VEIN K

5.12.1 Structural Controls and Geometry

Vein K occurs in the south west corner of the outcrop in the Pontiac metasedimentary rocks and forms sets with a relative spacing of 10-25cm. The veinlets are 0.5mm thick and consistently oriented at $110^{\circ}/85$. Vein K was classified as post- D_3 as it was seen to cross cut Vein J in the Pontiac metasedimentary rocks (Figure 13).

5.12.2 Mineralogy and Selvage Alteration

The Vein K system was not included in the selected samples for petrographic analysis from the outcrop or from drill core. Observations from outcrop classified the vein system as quartz veinlets 0.5mm thick. Pyrite precipitated in the veins causing them to be oxidized at surface. The vein system are in sharp contact with the surrounding host rock and no selvage alteration was observed.

5.13 GOLD CONTENT

Due to selective sampling at outcrop six of the eleven vein systems were analyzed for gold content.

Values for element determination using geochemical analysis were semi-quantitative due to the small sample weight used (0.5g) and the detection limit based on the analysis was 0.0002ppm. Results of the analysis can be seen in Table 2.

Table 2: Proportion of gold in selected vein systems determined by Aqua Regia- ICP analysis from ALS minerals.

Vein System	Host Rock	Gold Content (ppm)
Vein A	Pontiac metasedimentary rock	0.0015
Vein A	Pontiac metasedimentary rock	0.0005
Vein C	Pontiac metasedimentary rock	0.0042
Vein D	Intrusion	0.0053
Vein D	Intrusion	<0.0002
Vein F	Pontiac metasedimentary rock	0.0065
Vein H	Pontiac metasedimentary rock	0.0059
Vein H	Intrusion	0.3510
Vein I	Intrusion	0.0005
Vein J	Intrusion	0.0136
Vein J	Pontiac metasedimentary rock	0.0012

6 DISCUSSION

6.1 COMPARISON OF VEIN SYSTEMS

The main structural controls that were used to constrain the timing of the vein systems correlate to the main deformation events. These include the D_1 event, intrusion emplacement, the D_2 event and the D_3 event. Eleven vein systems were identified. The first three vein systems formed pre- D_2 . The fourth occurred after the quartz monzodiorite intrusion emplacement and formed pre- to syn- D_2 . The next five vein systems formed post- D_2 to pre- D_3 , whereas the final two veins systems occurred post- D_3 . This chronological sequence of vein-formation is summarized in Figure 30.

Vein System		D ₁ Event		D ₂ Event		D ₃ Event	
A	---	---	---	---			
B	---	---	---	---			
C	---	---	---	---			
D				—			
E					—		
F					—		
G					—		
H					—		
I					—		
J							—
K							—

Figure 30: Chronological sequence of the eleven vein systems found at the Cartier Zone. Veins A-C are denoted by hatch lines due to the lack of evidence to constrain the vein systems with either the D_1 event or the intrusion emplacement.

Among the veins that formed pre D_2 there were similarities in the modal abundance of quartz. The location of minor minerals within the vein systems and their contact with the Pontiac metasedimentary host rock are also criteria used to group them together. In Vein systems A, B and C, large quartz grains, constituting 85-90% of the vein, formed in the centre while minor proportions of feldspar and chlorite occurred at the contact in the vein margin (possibly as alteration products). Each of these vein systems are in sharp contact with the host rock. Vein C was the only pre- D_2 vein system to form a selvage which was comprised of quartz and feldspar.

Vein D was the only vein system to form largely syn- D_2 . Similar to the earlier vein systems, the modal abundance of quartz was high in Vein D and was comprised of 90% quartz with 10% carbonate occurring in the selvage of the vein. Of the quartz-carbonate veins that were characterized a Cartier Zone, Vein D was the only system to generate an alteration selvage. Comparisons were made between carbonate in the vein and carbonate replacement found in the intrusion. Due to similarities in colour and habit as well as the decrease in relative abundance distal to Vein D, it is proposed that a portion of the carbonate alteration that occurs in the intrusion was caused by the alteration attributed to the formation of the Vein D system.

Of the five vein systems that formed post- D_2 to pre- D_3 , two occurred in both rock types. Mineralogical compositions of Vein F and Vein H system are consistently similar between rock types. In the Pontiac Metasedimentary host rock the minor minerals formed at the vein margin, whereas in the intrusion they occurred closer to the center of the vein. Differences in vein thickness and orientation were observed between rock types in Vein F and H. This is due to the competency contrast between the quartz monzodiorite intrusion and the Pontiac metasedimentary rocks. There was a larger variation in mineralogical composition of the secondary minerals between vein systems while quartz remained the dominant mineralogical component.

The final two vein systems formed post-D₃. Both had quartz as the major mineralogical component. However, Vein J exhibited selvage alteration in both the Pontiac metasedimentary rocks and the porphyry intrusion whereas Vein K formed no selvage. Vein J formed biotite and chlorite replacement as well as zoned alteration of carbonate and muscovite in the intrusion. Due to similarities in colour, size, shape and relative abundance proximal to the vein system it is proposed that Vein J emplacement resulted in the formation of the pervasive biotite, chlorite, muscovite and carbonate alteration that is observed in the intrusion. However, more detailed studies in the outcrop and drill holes is needed to evaluate their broad spatial and temporal relationships.

Each of the vein systems found at Cartier Zone are in sharp contact with the surrounding host rock and have quartz as the dominant mineralogical component. However there appears to be no direct correlation between mineralogy and hydrothermal alteration with the timing of the vein systems. Alteration caused by the vein systems is more evident in the porphyry, creating wide spread pervasive alteration that extends beyond the vein selvage.

Geochemical analysis of the selected samples shows very little detectable gold associated with the vein systems. Generally the veins that occurred in the intrusion have higher gold values than veins found in the Pontiac metasedimentary rocks. The lowest detectable gold values of any of the samples came from the Vein I system that was comprised of quartz-tourmaline and the highest gold value was associated with the Vein H system that was comprised of quartz-pyrite. Based on the eleven samples that were analysed there appears to be no correlation between the content of gold and the relative timing of vein formation. However, more vein sampling and geochemical analysis is required to make a comprehensive geochemical comparison between vein systems.

6.2 COMPARISON WITH PREVIOUS WORK AT CARTIER ZONE

Comparing the eleven identified vein systems to previous work completed by Gunning and Ambrose (1940) as well as Neumayr et al. (2000), it is clear that there is a more complicated network of vein systems at Cartier Zone than previously noted. Gunning and Ambrose (1940) characterised one vein system as the quartz stockwork that crosscuts the porphyry and descriptions match those of the Vein D system. Neumayr et al. (2000) characterized five vein systems, four of which have broadly similar characteristics to the eleven vein systems that were identified in this study.

The V3A system that was identified by Neumayr et al. (2000) correlates to the Vein D system based on their description of the structural controls. Similarly, mineralogical composition and structural controls described by Neumayr et al. (2000) were used to correlate V3B to the Vein I system, V3C to the Vein H system and V3D to the Vein J system. There is a discrepancy in the chronological order of the V3B and V3C but observations from the field clearly showed Vein I crosscutting Vein H. Neumayr et al. (2000) only observed the Vein J system in the sediments however similarities in orientation and mineralogy prove that Vein J also occurs in the porphyry (Figure 31).

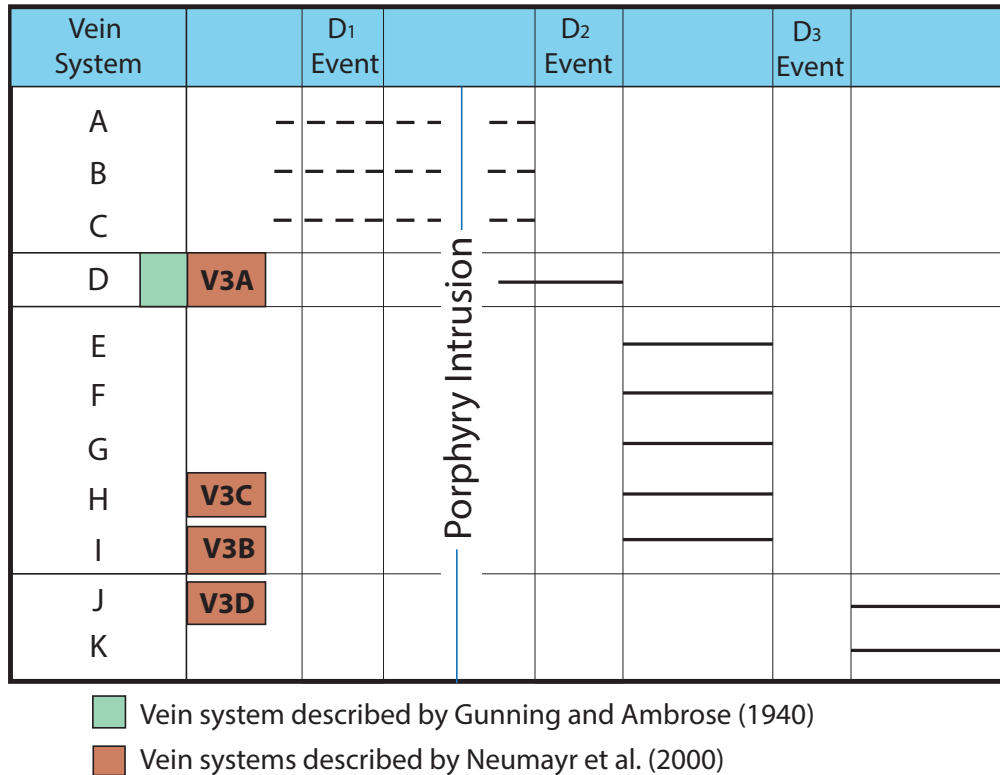


Figure 31: Vein chronology at Cartier Zone, comparing with the vein systems that were characterized previously.

Neumayr et al. (2000) identified that Vein Systems D, I, H and J contained pyrite mineralization in the selvage. However, both macroscopic and microscopic analysis from this study shows that pyrite is associated with the only the Vein H and J systems, and only forms in the selvage of Vein H. Neumayr et al. (2000) also reported that gold mineralization was associated with Vein systems D, I, and H. However, no geochemical assay was provided and geochemical analysis from this study shows that there is no detectable gold associated with both the Vein D and Vein I system and the highest proportion of gold (0.35 ppm) occurs in the Vein H system.

6.3 COMPARISON TO THE CANADIAN MALARTIC DEPOSIT

Intrusions hosting gold mineralization at the Canadian Malartic Deposit were interpreted to have formed syn-D₂ (2677–2679 Ma) where D₂ was characterized by a series of sub vertical, sub isoclinal folds

(Sanfaçon & Hubert, 1990). D₂ deformation described by Sansfaçon and Hubert (1990) corresponds to the D₂ deformation at Cartier Zone. The Vein D system that formed pre- to syn-D₂ was the most favorable system for gold mineralization however, results from the geochemical analysis showed Vein D, which formed pre- to syn-D₂, to have gold values of 0.0053ppm.

In the Canadian Malartic Deposit microscopic gold is associated with the main ore-stage alteration where pyrite, chalcopyrite, galena, sphalerite and hematite act as gold bearing phases (Sanfaçon & Hubert, 1990). These gold bearing phases exhibit strong spatial association with hydrothermal alteration and gold mineralization occurs in zones containing disseminated pyrite, widespread carbonate alteration, K-feldspar and biotite replacement and minor sericitization (Sanfaçon & Hubert, 1990). In addition fine-grained native gold is also present at the Canadian Malartic deposit and is associated with tellurides in quartz veins (Helt et al. 2014)

Examining the potential for gold bearing phases at the Cartier Zone, the proportion of pyrite and chalcopyrite is less than 1% and these occur predominantly in the Pontiac metasedimentary rocks. Galena, sphalerite and hematite were not observed in the host rock.

Hydrothermal alteration from the vein systems is restricted to the vein margins in the Pontiac metasedimentary rocks. Of the six vein systems in the intrusion, only two form weak pervasive alteration as carbonate, biotite, chlorite and muscovite replacement and constitutes only 10-15% of the modal mineralogy in the intrusion in the vein wall.

Important alteration assemblages like potassium feldspar replacement and sericitization were not observed in Cartier Zone and pyrite mineralization is only present within two vein systems and occurs at the margins of the veins of in the immediate selvage. Silicification occurs in the intrusion at the contact with the Pontiac metasedimentary rocks separate from the weak pervasive alteration caused by the vein

emplacement. Carbonate and biotite replacement does occur in the intrusion however it only constitutes 10-15% of the modal abundance, replacing the quartz groundmass.

When examining mineralogical composition and alteration, indicating features that are required for gold mineralization that occur at the Canadian Malartic Deposit are either not present or may have been destroyed at Cartier Zone.

A comparison with the vein systems observed at the Canadian Malartic Deposit and Cartier Zone was conducted based on mineral assemblages (Helt et al., 2014). The quartz \pm feldspar \pm chlorite veins that formed pre D_2 and the quartz-carbonate vein system that formed pre- to syn- D_2 appear to be associated with the early pre ore-stage veins that formed at the Canadian Malartic Deposit.

At the Canadian Malartic Deposit the early stage alteration replaced the groundmass of the intrusion and the Pontiac metasedimentary rock with quartz and carbonate (De Souza, 2014). Although silicification is not attributed to the earlier vein systems at Cartier Zone, weak pervasive carbonate alteration from the Vein D system occurs in the intrusion. The quartz-carbonate and quartz-pyrite vein systems that formed Post D_2 in both the Pontiac metasedimentary host rock and the quartz monzodiorite intrusion are most likely associated with the pre ore-stage veins seen at the Canadian Malartic Deposit.

7 CONCLUSION AND FURTHER WORK

Eleven different vein systems were characterized at Cartier Zone which is more than what was described by Gunning and Ambrose (1940) and Neumayr et al. (2000). Vein systems were classified in chronological order due to cross cutting relationships observed at outcrop and drill core logging. Vein systems A, B and C formed pre-D₂ and occur in the Pontiac metasedimentary rocks. The Vein D system, classified as pre- to syn-D₂, is the first vein system to form in the intrusion. Vein systems E, F, G, H formed post-D₂ and pre-D₃ and occur in both the Pontiac metasedimentary rock and the intrusion. The Vein J system occurs in both rock types and formed post-D₃ while the Vein K system formed post-D₃ and was restricted to the Pontiac metasedimentary rocks.

All vein systems are in sharp contact with the host rock and with the exception of Vein E that was composed entirely of plagioclase, quartz was the primary mineralogical constituent in each of the vein systems. Minor proportions of ± carbonate, ± feldspar, ± chlorite, ± biotite, and ± pyrite and ± tourmaline formed in the margin of the veins. Vein E in the Pontiac metasedimentary rocks and Veins D, H and J in the intrusion developed notable alteration selvages. Weak pervasive alteration in the form of carbonate, biotite, chlorite and muscovite replaced the quartz groundmass in the intrusion and accounted for 5-10% of the modal abundance. A portion of the carbonate alteration is attributed to the emplacement of the Vein D and J systems while Vein J is also attributed to the weak pervasive biotite, chlorite muscovite alteration.

The quartz ± feldspar ± chlorite veins that formed pre-D₂ and the quartz-carbonate vein system that formed pre- to syn-D₂ appear to be associated with the early pre ore-stage veins at the Canadian Malartic Deposit, whereas The quartz-carbonate and quartz-pyrite vein systems that formed Post-D₂ in both the Pontiac metasedimentary host rock and the quartz monzodiorite intrusion are most likely

associated with the pre ore-stage veins seen at the Canadian Malartic Deposit. Specific indicating features required for gold mineralization that occur at the Canadian Malartic Deposit in the form of mineralogical composition and alteration are either not present or may have been destroyed at Cartier Zone.

Further work needs to be completed to determine the chemical composition of specific minerals.

Microprobe analysis is needed for Vein systems D, F and J to determine the chemical composition of carbonate in the vein system to distinguish whether it is calcite or ankerite. This is important to improve correlation of the vein systems at Cartier Zone to the Canadian Malartic Deposit. Similarly, Vein systems A, C and E need to be examined for the chemical composition of the feldspar that occurs in the margin of the vein to determine whether it is alkali. In addition microprobe would be beneficial to determine the chemistry of the biotite that forms the main S_2 foliation in the Pontiac metasedimentary rocks.

When examining the gold content of the vein systems only eleven samples that were analysed. In order to make an accurate correlation between the content of gold and the relative timing of vein formation, more vein sampling and geochemical analysis is required.

The proposal that the emplacement of Vein D and Vein J caused the weak carbonate alteration of the intrusion was based exclusively on optical observations so a geochemical comparison using microprobe analysis is required to see if the carbonate alteration originated from the Vein D or the Vein J system. In addition to the geochemical analysis more detailed studies in the outcrop and drill holes is needed to evaluate the broad spatial and temporal relationships. This approach should also be taken to examine biotite, chlorite and muscovite alteration in the porphyry to see if it is derived from the Vein J system.

8 REFERENCES

- Corfu, F. (1993). The evolution of the southern Abitibi Greenstone Belt in light of precise U-Pb geochronology. *Economic Geology* , 88, 1323-1340.
- Corfu, F., Krogh, T., Kwok, Y., & and Jensen, L. (1989). U-Pb zircon geochronology in the southwestern Abitibi greenstone belt, Superior Province. *Canadian Journal of Earth Sciences* , 26, 1747-1763.
- Davis, D. (2002). U–Pb geochronology of Archean metasedimentary rocks in the Pontiac and Abitibi subprovinces, Quebec, constraints on timing, provenance and regional tectonics. *Precambrian Research* , 115, 97-117.
- Davis, D. (1992). U-Pb dating of detrital zircon in sediments in the Pontiac and Abitibi subprovinces; preliminary results. *19*, 33-55.
- Davis, W., Lacroix, S., Gariépy, C., & Machado, N. (2000). Geochronology and radiogenic isotope geochemistry of plutonic rocks from the central Abitibi subprovince: Significance to the internal subdivision and plutono- tectonic evolution of the Abitibi belt. *Canadian Journal of Earth Sciences* , 37, 117-133.
- De Souza, S. (2014). The world-class Canadian Malartic deposit: a multi-stage porphyry associated low-grade bulk-tonnage Archean gold deposit, Southern Abitibi, Québec. *Society of Economic Geology (Abstract)* .
- Desrochers, J., & Hubert, C. (1996). Structural evolution and early accretion of the Archean Malartic Composite Block, southern Abitibi greenstone belt, Quebec, Canada. *Canadian Journal of Earth Sciences: Natural Resources Canada* , 33, 1556-1569.

- Dubé, B., & Gosselin, P. (2007). Greenstone-hosted quartz-carbonate vein deposits. Mineral Deposits of Canada: A synthesis of major deposit types, district metallogeny, the evolution of geological provinces and exploration methods. *Geological Association of Canada* , 5, 49-73.
- Gunning, J., & Ambrose, H. (1940). Malartic Area, Quebec: Memoir 222. *Canadian Department of Mines and Resources* , 40-50.
- Helt, K., Williams-Jones, A., Clark, J., Wing, B., & Wares, R. (2014). Constraints on the Genesis of the Archean Oxidized, Intrusion-Related Canadian Malartic Gold Deposit, Quebec, Canada. *Economic Geology* , 109, 713-735.
- Lajoie, L., & J, L. (1984). Petrology of the Archean Pontiac and Kewagama sediments and implications for the stratigraphy of the southern Abitibi belt. *Canadian Journal of Earth Sciences* , 21, 1305-1314.
- Minerals, A. (2009, April). *Trace level methods using conventional ICP-AES analysis*. Retrieved April 2015 from Geochemical Procedure: ME ICP41: www.alsglobal.com/.../Minerals/.../ME-ICP41%20Aqua%20Regia- ICP%20Multi-element%20Method.pdf
- Neumayr, P., Hagemann, S., & Couture, J. (2000). Structural setting, textures, and timing of hydrothermal vein systems in the Val d'Or camp, Abitibi, Canada: implications for the evolution of transcrustal, second-and third-order fault zones and gold mineralization. *Canadian Journal of Earth Sciences* , 37, 95-114.
- Powell, W., Carmichael, D., & Hodgson, C. (1995). Conditions and timing of metamorphism in the southern Abitibi greenstone belt, Quebec. *Canadian Journal of Earth Sciences* , 32, 787-805.
- Robert, F. (1997). A preliminary geological model for syenite associated disseminated gold deposits in the Abitibi belt, Ontario and Quebec. *Geologic Survey of Canada* , 201-210.

Robert, F. (1989). Internal structure of the Cadillac tectonic zone southeast of Val d'Or, Abitibi greenstone belt, Quebec. *Canadian Journal of Earth Sciences* , 26, 2661-2675.

Robert, F. (1990). Structural setting and control of gold-quartz veins of the Val d'Or area, southeastern Abitibi subprovince. *University of Western Australia* , 24, 167-209.

Robert, F. (2001). Syneite-associated gold deposit in the Abitibi greenstone belt, Canada. *Mineralium Deposita* , 36, 503-516.

Sanfaçon, R., & Hubert, C. (1990). The Malartic Gold District, Abitibi greenstone belt, Québec: Geological setting, structure and timing of gold emplacement Barnat, East- Malartic, Canadian Malartic and Sladen Mines, in Rive, M., and Verpaelst, P., eds., The northwestern Quebec polymetallic belt: A summary of 60 years of mining exploration. *Canadian Institute of Mining and Metallurgy* , 43, 221-235.

Wares, R., & Burzynski, J. (2012). *The Canadian Malartic Mine, Southern Abitibi Belt, Quebec, Canada: Discovery and Development of an Archean Bulk-Tonnage Gold Deposit*. Montreal: Osisko Mining Corporation.

Whitney, D., & Evans, B. (2010). Abbreviation for names of rock-forming minerals. *American Mineralogists* , 95, 185-187.

Winchester, J. a. (1977). Geochemical discrimination of different magma series and their differentiation products using immobile elements. *Chemical Geology* , 20, 325-343.